Title

Actin cytoskeleton—dependent regulation of corticotropin-releasing factor receptor heteromers

Journal

Molecular Biology of the Cell, 28(18)

ISSN

1059-1524

Authors

Hasdemir, Burcu

Mahajan, Shilpi

Oses-Prieto, Juan

et al.

Publication Date

2017-09-01

DOI

10.1091/mbc.e16-11-0778

Peer reviewed

Actin cytoskeleton–dependent regulation of corticotropin-releasing factor receptor heteromers

Burcu Hasdemir[a,b], Shilpi Mahajan[c], Juan Oses-Prieto[d], Shreya Chand[d], Michael Woolley[e], Alma Burlingame[d], Dimitris K. Grammatopoulos[e], and Aditi Bhargava[a,b,c,*]

[a]Osher Center for Integrative Medicine, [b]Department of Obstetrics & Gynecology, [c]Department of Surgery, and [d]Departments of Pediatrics, Pharmacology, and Chemistry, University of California, San Francisco, San Francisco, CA 94143; [e]Translational and Systems Medicine, Warwick Medical School, University of Warwick, Coventry CV4 7AL, UK

ABSTRACT **Stress responses are highly nuanced and variable, but how this diversity is achieved by modulating receptor function is largely unknown. Corticotropin-releasing factor receptors (CRFRs), class B G protein–coupled receptors, are pivotal in mediating stress responses. Here we show that the two known CRFRs interact to form heteromeric complexes in HEK293 cells coexpressing both CRFRs and in vivo in mouse pancreas. Coimmunoprecipitation and mass spectrometry confirmed the presence of both CRF_1R and $CRF_2\beta R$, along with actin in these heteromeric complexes. Inhibition of actin filament polymerization prevented the transport of $CRF_2\beta R$ to the cell surface but had no effect on CRF_1R. Transport of CRF_1R when coexpressed with $CRF_2\beta R$ became actin dependent. Simultaneous stimulation of cells coexpressing CRF_1R+$CRF_2\beta R$ with their respective high-affinity agonists, CRF+urocortin2, resulted in approximately twofold increases in peak Ca^{2+} responses, whereas stimulation with urocortin1 that binds both receptors with 10-fold higher affinity did not. The ability of CRFRs to form heteromeric complexes in association with regulatory proteins is one mechanism to achieve diverse and nuanced function.**

Monitoring Editor
Carl-Henrik Heldin
Ludwig Institute for Cancer Research

Received: Nov 14, 2016
Revised: Jun 30, 2017
Accepted: Jul 7, 2017

INTRODUCTION

At any given time, a cell expresses several different G protein–coupled receptors (GPCRs), which enables it to respond to a plethora of extracellular agonists in a spatiotemporal manner. Many GPCRs do not operate in isolation, but may "talk" to other receptors and proteins via physical association for an integrated and balanced response to different stimuli (Vischer *et al.*, 2011). GPCR heteromerization can often modify functional characteristics of the individual monomers, including subcellular localization, agonist binding, and downstream signaling (Levoye *et al.*, 2006; Springael *et al.*, 2007; Milligan, 2009; Vischer *et al.*, 2011). Though most GPCR monomers have the capacity to elicit an intracellular signaling response upon agonist binding, many GPCRs exist and function as homomeric or heteromeric assemblies. For example, the umami and sweet taste receptors (TIR) are heterodimeric assemblies of T1R3 in combination with T1R1 or T1R2, respectively (Zhao *et al.*, 2003). Also, constitutive homodimerization of class B secretin receptors was found to facilitate G-protein coupling, which is critical for secretin binding (Harikumar *et al.*, 2006; Gao *et al.*, 2009). GPCRs are also known to interact with accessory proteins known as receptor activity–modifying proteins (RAMPs). RAMPs regulate the activities of several GPCRs, including the receptors for secretin, calcitonin, glucagon, and vasoactive intestinal peptide (Sexton *et al.*, 2006). Interaction of RAMPs with GPCRs can modulate receptor actions, including chaperoning of the receptor to the cell surface, as is the case for the calcitonin receptor-like receptor. RAMP present in a heterodimer

This article was published online ahead of print in MBoC in Press (http://www.molbiolcell.org/cgi/doi/10.1091/mbc.E16-11-0778) on July 12, 2017.

Conflict of interest: The authors have nothing to disclose.

Author contributions: A. Bhargava conceptualized and coordinated the study, analyzed the data, and wrote the paper. B.H. and S.M. performed experiments, analyzed the data, and wrote parts of the paper. J.O.-P. and S.C. performed experiments and analyzed the data. A. Burlingame supervised MS experiments. D.K.G. provided FL-$CRF_2\beta R$, edited the manuscript, and together with M.W. performed and analyzed cAMP assays.

*Address correspondence to: Aditi Bhargava (Aditi.Bhargava@ucsf.edu).

Abbreviations used: BSA, bovine serum albumin; Co-IP, coimmunoprecipitation; CRF, corticotropin-releasing factor; CRF_1R, corticotropin-releasing factor receptor 1; CRF_2R, corticotropin-releasing factor receptor 2; CRFR, CRF receptor; ER, endoplasmic reticulum; FITC, fluorescein isothiocyanate; GPCR, G protein–coupled receptor; HA, hemagglutinin; Hsp70, heat shock protein 70; IgG, immunoglobulin G; IP, immunoprecipitation; LC-MS/MS, liquid chromatography–electrospray tandem MS; MS, mass spectrometry; PAR_2, protease-activated receptor 2; PBS, phosphate-buffered saline; RAMP, receptor activity–modifying protein; SP, signal peptide; Ucn1, urocortin 1; Ucn2, urocortin 2.

may modulate other functions, such as receptor internalization and recycling and downstream signaling pathways (Sexton *et al.*, 2006).

Stress responses to the same stressor are highly individualized and nuanced. An ancient family of neuropeptide hormones known as the corticotropin-releasing factor (CRF) family that comprises four known agonists, CRF and urocortins (Ucn1–3), mediates stress responses. The neuropeptide hormone CRF is primarily responsible for regulating and/or initiating stress responses via activation of the hypothalamic–pituitary–adrenal axis (Muglia *et al.*, 1995), whereas urocortins play a vital role in the recovery response to stress (Neufeld-Cohen *et al.*, 2010). These neuropeptides mediate their effect via two known class B GPCRs, CRF_1R and CRF_2R. CRF_2R has three splice variants in humans: $CRF_2\alpha R$, $CRF_2\beta R$, and $CRF_2\gamma R$. CRF_1R and CRF_2R have different agonist binding affinities as determined using in vitro binding assays. CRF has a relatively higher affinity for CRF_1R compared with CRF_2R. Ucn1 has equal affinity for both receptors, but a 10-fold higher binding affinity than that displayed by CRF, and Ucn2 and Ucn3 are selective for CRF_2R (Vaughan *et al.*, 1995; Lewis *et al.*, 2001; Reyes *et al.*, 2001).

Stressors activate both CRF_1R and CRF_2R receptors. CRF_1R activation mediates adrenocorticotropic hormone release, anxiety-like behavior, and short-term anorexia, whereas CRF_2R activation mediates stress-coping responses, including anxiolytic behavior and long-term anorexia (Hotta *et al.*, 1999; Reyes *et al.*, 2001). Acute stress induces a comprehensive and integrated response to maintain homeostasis and survival of organisms. The absence of proper counterregulation might lead to exaggerated stress responses and detrimental consequences for the organism (Chrousos, 2009). Therefore, the counterbalancing actions of CRF_2R might be critical under a stressful condition. Many organs and cell-types coexpress both CRF receptors, which function "hand-in-hand" for an integrated response to stress and to bring the system back to homeostatic baseline (Bhargava, 2011; Henckens *et al.*, 2016).

CRF_1R is known to hetero(di)merize with vasopressin receptor V1b to mediate synergistic actions of vasopressin and CRF (Murat *et al.*, 2012). As a heteromeric partner of $5HT_{2A/C}Rs$, CRF_1R responds to serotonin to signal via inositol triphosphate (Magalhaes *et al.*, 2010). CRF_1R is known to harbor a cleavable signal peptide (SP) (Rutz *et al.*, 2006; Schulz *et al.*, 2010) and exists in an equilibrium state of monomer/dimer that is already established in the endoplasmic reticulum (ER) (Teichmann *et al.*, 2014). $CRF_2\alpha R$, on the other hand, harbors a pseudo-SP that is thought to prevent receptor oligomerization (Teichmann *et al.*, 2012). Deletion of the SP of $CRF_2\alpha R$ results in receptors being trapped in the ER (Rutz *et al.*, 2006). It remains to be established whether $CRF_2\beta R$ harbors a functional or pseudo-SP.

Recently we have shown that a balanced and coordinated expression of CRF receptors is required for actions of Ucn3 at baseline and during inflammation (Mahajan *et al.*, 2014), but it remains to be established whether this effect on physiological function involves physical interaction between CRF receptors and formation of heteromeric complexes. In this study we determine whether CRF receptors form heteromeric complexes and the functional significance of this association.

RESULTS

CRF2βR shows both cell surface and intracellular expression

The cellular location of a given GPCR determines its function. Using an antibody that recognizes the C-terminus of both CRF_1R and CRF_2R (anti-$CRFR_{1/2}$), we have previously shown that CRF_1R expressed in HEK293 cells localized mainly to the plasma membrane (Hasdemir *et al.*, 2012). We now examined the localization of $CRF_2\beta R$ expressed in HEK293 cells and found this receptor to be present both at the cell surface and intracellular compartments, irrespective of whether the cells were transiently or stably transfected (Figure 1A). To characterize whether $CRF_2\beta R$ from the cell surface internalizes with bound agonist, we first used fluorescently labeled agonists: 5-carboxyfluorescein–labeled Ucn1 (5-FAM-Ucn1) and Rhodamine Red–labeled CRF (Rhod-CRF). HEK293 cells expressing CRF_1R were used as positive controls, as Ucn1 is known to bind both CRFRs with equal affinity in in vitro assays (Vaughan *et al.*, 1995). Untransfected HEK293 cells were used as negative controls. The 5-FAM-Ucn1 bound strongly to cell surface $CRF_2\beta R$ and CRF_1R (Figure 1, B and C, top panels) and the agonist-bound receptors internalized to endosomes within 30 min of incubation (Figure 1, B and C, bottom panels). Cell surface $CRF_2\beta R$ did not bind appreciably to Rhod-CRF and did not show any appreciable internalization after 30 min of incubation, whereas CRF_1R bound to Rhod-CRF showed robust internalization within 30 min of incubation (Figure 1, E and F). Importantly, untransfected HEK293 cells did not bind 5FAM-Ucn1 or Rhod-CRF, nor did they show any discernible expression of CRFRs (Figure 1, D–G). These results further confirm in vitro observations that Ucn1 binds to both CRF_1R and CRF_2R and takes it a step further to show that ligand-bound receptors *are* internalized.

CRF2βR harbors a cleavable SP

While the SPs for CRF_1R and $CRF_2\alpha R$ have been studied before (Alken *et al.*, 2005; Rutz *et al.*, 2006; Schulz *et al.*, 2010; Teichmann *et al.*, 2012), it is unknown whether $CRF_2\beta R$ harbors a pseudo- or cleavable SP. Using the Max Planck Institute proteasome cleavage prediction site (www.mpiib-berlin.mpg.de/mpiib-cgi/MAPPP/cleavage.pl), we identified putative cleavage domains within the first 33 amino acids (Figure 2A). On the basis of this plot and the putative cleavage site for $CRF_2\alpha R$ (Perrin *et al.*, 2003), we constructed a Flag-tagged delta(Δ)SP version of $CRF_2\beta R$ (Flag-$CRF_2\beta R\Delta SP$) lacking the N-terminal 26 amino acids and N-terminal hemagglutinin (HA)–tagged and Flag-tagged full-length $CRF_2\beta R$ (HA-$CRF_2\beta R$ and Flag- $CRF_2\beta R$). Schematic representations of all tagged constructs used in this study are shown in Figure 2B. Construction of HA-tagged CRF_1R (HA-CRF_1R) was described by us elsewhere (Hasdemir *et al.*, 2012). In HEK293 cells expressing HA-$CRF_2\beta R$ or Flag- $CRF_2\beta R$, we were unable to detect the full-length receptor using anti-HA or anti-Flag antibodies, whereas the anti-$CRFR_{1/2}$ antibody that recognizes the C-terminus of CRFRs clearly detected both the HA- and Flag- tagged $CRF_2\beta R$ both at the cell surface and in intracellular compartments (Figure 2C). Only intracellular staining was detected with the anti-HA antibody (Figure 2C, arrowheads), whereas the Flag tag was not detected at all, suggesting that the N-terminal tags are cleaved off from the nascent peptide. On the other hand, Flag-$CRF_2\beta R\Delta SP$ was detected with both anti-Flag and anti-$CRFR_{1/2}$ antibodies at the cell surface (Figure 2D). HA-tagged CRF_1R was used as a positive control, and its expression was detected at the cell surface using both anti-HA and anti-$CRFR_{1/2}$ antibodies (Figure 2E). When primary antibody was omitted, no staining was seen (Figure 2E, bottom panel). These data suggested that the N-terminal SP of $CRF_2\beta R$ is cleavable.

Next we confirmed that HEK293 cells expressing either HA-$CRF_2\beta R$ or Flag-$CRF_2\beta R\Delta SP$ showed similar subcellular localization of the receptors both under basal unstimulated and agonist-stimulated conditions (Figure 3, A and B). Under unstimulated conditions, both the full-length and ΔSP versions of $CRF_2\beta R$ showed both cell surface and intracellular localization. Stimulation with Ucn1, a high-affinity agonist, or Ucn2, a lower-affinity but CRF_2R-specific agonist, resulted in internalization of $CRF_2\beta Rs$ (Figure 3, A and B, middle and

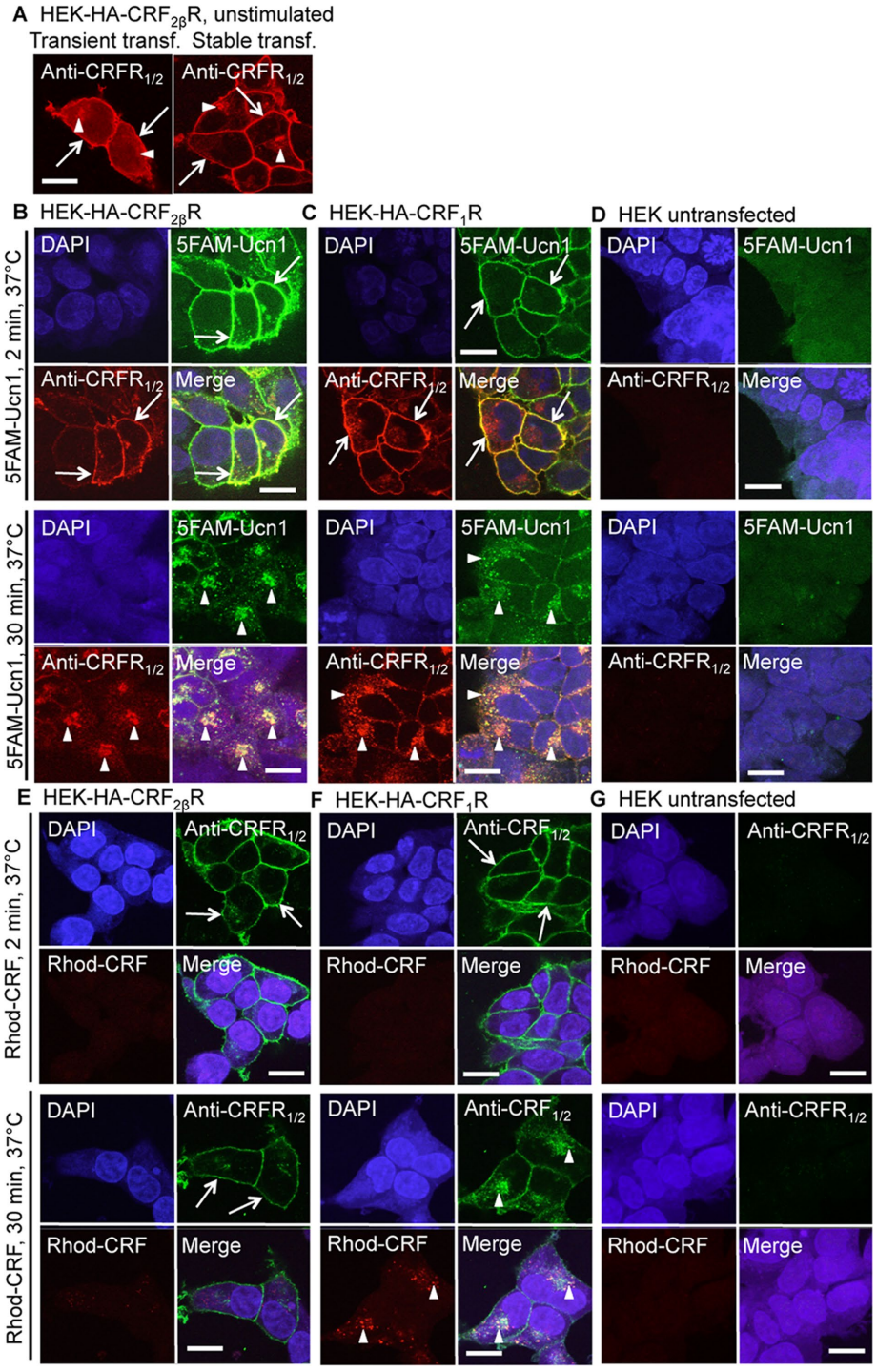

FIGURE 1: $CRF_2\beta R$ shows both cell surface and intracellular localization. (A) HEK293 cells transiently or stably expressing $CRF_2\beta R$ were seeded on coverslips and 48 h later fixed and immunostained. Using an antibody that recognizes the C-terminus of CRF receptors (anti-$CRFR_{1/2}$), we found that $CRF_2\beta R$ localizes to both the cells surface (arrows) and to intracellular compartments (arrowheads). (B) HEK293 cells stably expressing $CRF_2\beta R$ were incubated with 5-carboxyfluorescein–labeled Ucn1 (5-FAM-Ucn1; 100 nM) for 2 and 30 min and immunostained with anti-$CRFR_{1/2}$ antibody (secondary antibody RRX) as in A, and images were captured on a Zeiss confocal microscope. At 2 min, Ucn1-bound $CRF_2\beta Rs$ were predominantly found at the plasma membrane (arrows). At 30 min, Ucn1-bound $CRF_2\beta Rs$ co-internalized and showed predominantly intracellular localization (arrowheads). (C) Similarly, HEK293 cells stably expressing CRF_1R were incubated with 100 nM 5-FAM-Ucn1 for 2 and 30 min and immunostained with anti-$CRF_{1/2}$ antibody (secondary antibody RRX) as in B. At 2 min, Ucn1-bound CRF_1Rs were predominantly found at the plasma membrane (arrows). At 30 min, Ucn1-bound CRF_1Rs co-internalized and showed predominantly intracellular localization (arrowheads). (D) HEK293 cells (untransfected) were incubated with 5-FAM-Ucn1 and processed as in B and C. The 5-FAM-Ucn1 did not show any nonspecific binding. (E) HEK293 cells stably expressing $CRF_2\beta R$ were incubated with 100 nM of Rhodamine Red–labeled CRF (Rhod-CRF; 100 nM) for 2 and 30 min and processed as in B, except that the secondary antibody used was FITC labeled. At 2 and 30 min, no appreciable binding of Rhod-CRF was observed (lack of any red staining), and $CRF_2\beta R$ was predominantly found at the plasma membrane (green, arrows). (F) Similarly, HEK293 cells stably expressing CRF_1R were incubated with Rhod-CRF and processed as in E. At 2 min of incubation, little if any Rhod-CRF bound to CRF_1R, and the receptors were predominantly found at the plasma membrane (arrows). After 30 min of incubation, Rhod-CRF–bound CRF_1R co-internalized and showed intracellular localization (arrowheads). (G) Untransfected HEK293 cells were incubated with Rhod-CRF and processed as in E and F. Importantly, Rhod-CRF did not show any nonspecific binding. Scale bar: 10 μm. Representative images are shown ($n = 2$ coverslips per condition, and each experiment was performed three times).

bottom panels). Quantification of the confocal images demonstrates that, in unstimulated cells, the cell surface expression of both $CRF_2\beta R$ constructs was equivalent (Figure 3C). Western blot analysis further confirmed that both $CRF_2\beta R$ constructs were equally expressed (Figure 3D).

Next we ascertained whether deletion of SP of $CRF_2\beta R$ alters function. The CRF receptors signal via coupling to several G proteins to increase intracellular cAMP levels (Reisine *et al.*, 1985; Grammatopoulos, 2012) and/or Ca^{2+} levels (Hasdemir *et al.*, 2012). We confirmed that the intracellular increase in cAMP and Ca^{2+} levels mediated by unmodified $CRF_2\beta R$ and $CRF_2\beta R\Delta SP$ were similar after Ucn1 or Ucn2 stimulation (Figure 3, E and F). This suggests that the cleavage of SP of $CRF_2\beta R$ does not affect internalization or downstream signaling ability in the systems examined and that the SP is cleaved to obtain a functional receptor.

Identification of CRF receptor heteromeric complex and CRFR-interacting proteins by mass spectrometry analysis

Heteromerization of CRF_1R with CRF_2R has not been previously demonstrated. CRF_1R is shown to exist as a monomer or homo(di)mer (Teichmann *et al.*, 2014), whereas the pseudo-SP of $CRF_2\alpha R$ is thought to prevent

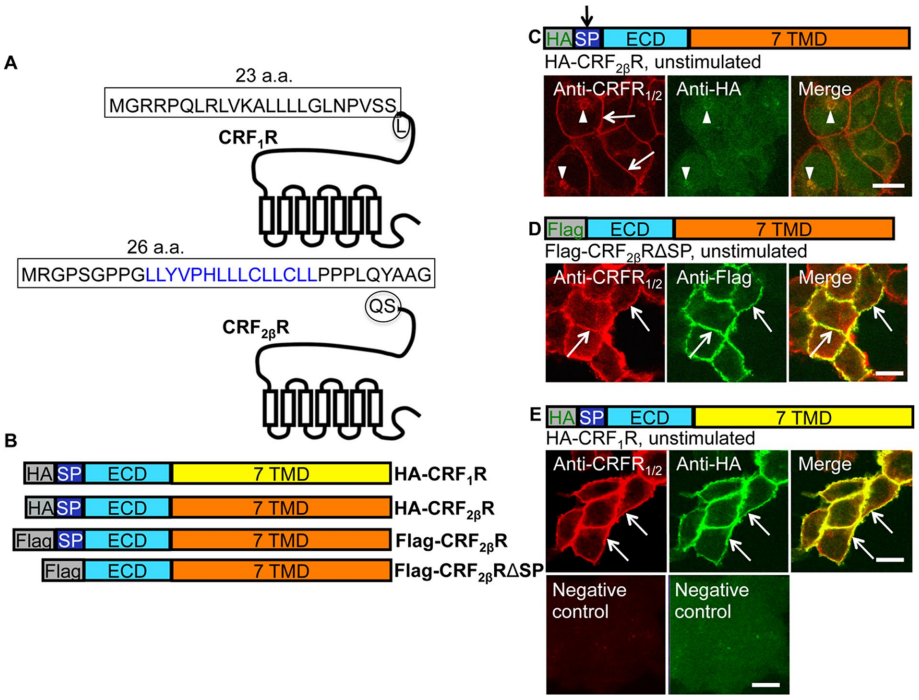

FIGURE 2: $CRF_2\beta R$ harbors a cleavable N-terminal SP. (A) A putative SP of $CRF_2\beta R$ contained within the first 33 amino acids (aa) was identified based on the Max Planck Institute proteasome cleavage prediction site. The maximum cleavage probability lies within the first 26 amino acids, in the domain: LLYVPHLLLCLLCL (blue text). The known SP of CRF_1R is contained within the first 23 aa. (B) Schematic representations of N-terminal epitope-tagged constructs used in this study are shown. (C) In HEK293 cells stably expressing HA-$CRF_2\beta R$, anti-$CRFR_{1/2}$ antibody detected the receptor both at the cell surface (arrows) and in intracellular compartments (arrowheads), whereas anti-HA antibody showed only intracellular staining (arrowheads), suggesting that the HA tag is cleaved from the nascent receptor. (D) In HEK293 cells stably expressing Flag-$CRF_2\beta R\Delta SP$, both anti-$CRFR_{1/2}$ and anti-Flag antibodies detected the receptor at the cell surface (arrows). (E) In HEK293 cells stably expressing HA-CRF_1R, both anti-$CRFR_{1/2}$ and anti-HA antibodies detected the receptor at the cell surface (arrows). In the absence of primary antibody (negative control), no staining was visible (bottom). Scale bar: 10 µm. Representative images are shown ($n = 2$ coverslips per condition, and each experiment was performed three times).

oligomerization (Teichmann *et al.*, 2012). For ascertaining whether CRF receptors are capable of physically interacting and forming heteromeric complexes, HEK293 cells were transfected with HA-CRF_1R or Flag-$CRF_2\beta R\Delta SP$ alone or cotransfected with both HA-CRF_1R+Flag-$CRF_2\beta R\Delta SP$. Western blot analysis using anti-$CRFR_{1/2}$ antibody that detects both receptors (Chang *et al.*, 2011) revealed the presence of CRFR monomers (at ~75 kDa) and a CRFR multimeric complex (at ~250 kDa) that were not present in untransfected HEK293 cells (Figure 4A). In HEK293 cells cotransfected with both CRFRs, only a ~250 kDa band was detected, which suggested that CRF_1R and $CRF_2\beta R\Delta SP$ resolve on SDS–PAGE as a multimeric protein complex, as has been reported for other GPCRs (Vischer *et al.*, 2015). To ensure that receptor heteromerization was not restricted to transfected HEK cells, but is a phenomenon that occurs in vivo, without cotransfection in tissues known to express both CRF receptors (pancreas) or only CRF_2R (colon), we used protein lysates from pancreas and colon tissue to demonstrate presence of a higher molecular band in tissue coexpressing both receptors. We observed the presence of an ~250 kDa band, along with CRFR monomers and homo- and/or heterodimers in pancreatic tissue lysates from mice, whereas only CRFR monomers and dimers were present in colonic lysates (Figure 4B).

For further investigation of the CRF_1R+$CRF_2\beta R$ interaction and identification of other interacting partners in the receptor supercomplex, HEK293 cells coexpressing epitope-tagged CRFRs (HA-CRF_1R+Flag-$CRF_2\beta R\Delta SP$) were stimulated with CRF, and the complex was purified. In the absence of well-characterized antibodies that distinguish between CRF receptors, anti-HA antibodies were used to pull down complexes (Figure 4C) and identify interacting partners using mass spectrometry (MS), an approach used previously by others and by us (Bockaert *et al.*, 2004; Gingras *et al.*, 2005; Trester-Zedlitz *et al.*, 2005). Immunoprecipitated complexes were separated by SDS–PAGE (Figure 4C), excised and digested with trypsin, and subjected to analysis by reverse-phase liquid chromatography–electrospray tandem MS (LC-MS/MS). MS analysis of the proteins that coprecipitated with HA-tagged HA-CRF_1R in cells coexpressing Flag-$CRF_2\beta R\Delta SP$ revealed hundreds of proteins (Supplemental Table 1). Several of the proteins that interacted with CRFR complex were specifically enriched compared with pull downs of untransfected (mock) cells (Figure 4D). As expected, MS analysis detected CRF_1R receptor in the multimeric receptor–protein complex and confirmed the presence of $CRF_2\beta R$ in HEK293 cells coexpressing both CRFRs and stimulated with CRF (Figure 4D and Supplemental Table 1). A number of cytoskeleton-associated proteins, including F-actin and filament A, interact with the i3 loop of GPCRs (Binda *et al.*, 2002; Cornea-Hebert *et al.*, 2002; Kim *et al.*, 2002). GPCRs undergoing endocytosis require cytoskeletal support to mediate trafficking. Several proteins critical for trafficking of receptors and maintaining cell structure and integrity were coimmunoprecipitated with CRFRs and were specifically enriched in receptor complexes according to the abundances in immunoprecipitated complex estimated by spectral counting. These proteins included tubulin α/β-chain, actin, and heat shock protein 70 (Hsp70) proteins (Figure 4D and Supplemental Table 1).

To confirm these MS findings and to explore agonist-specific interactions of CRF_1R with $CRF_2\beta R$ and the possibility of simultaneous receptor activation in presence of multiple agonists, we stimulated HEK293 cells coexpressing both receptors with CRF, Ucn2, or Ucn1 alone, or a cocktail of CRF+Ucn2. Immunoprecipitation (IP) of HA-CRF_1R was performed using anti-HA antibodies and separated by SDS–PAGE. As expected, agonist treatment did not affect the presence of HA-CRF_1R in HEK293 cells coexpressing both CRF receptors (Figure 4E). Western blot analysis with anti-Flag antibody confirmed that Flag-$CRF_2\beta R\Delta SP$ was coimmunoprecipitated with HA-CRF_1R (Figure 4F). Additionally, actin was found to interact with the CRF receptor complex (Figure 4F, blots 1 and 2, and Supplemental Figure S1A) and was not present in the co-IP complex from HEK cells alone, although actin was present in inputs from all conditions. We used protease-activated receptor 2 (PAR_2), another GPCR (Hasdemir *et al.*, 2007) that is unrelated to the CRF family in its function to validate that actin is a specific interacting partner for CRFRs. HEK cells expressing PAR_2 with an N-terminal Flag epitope and a

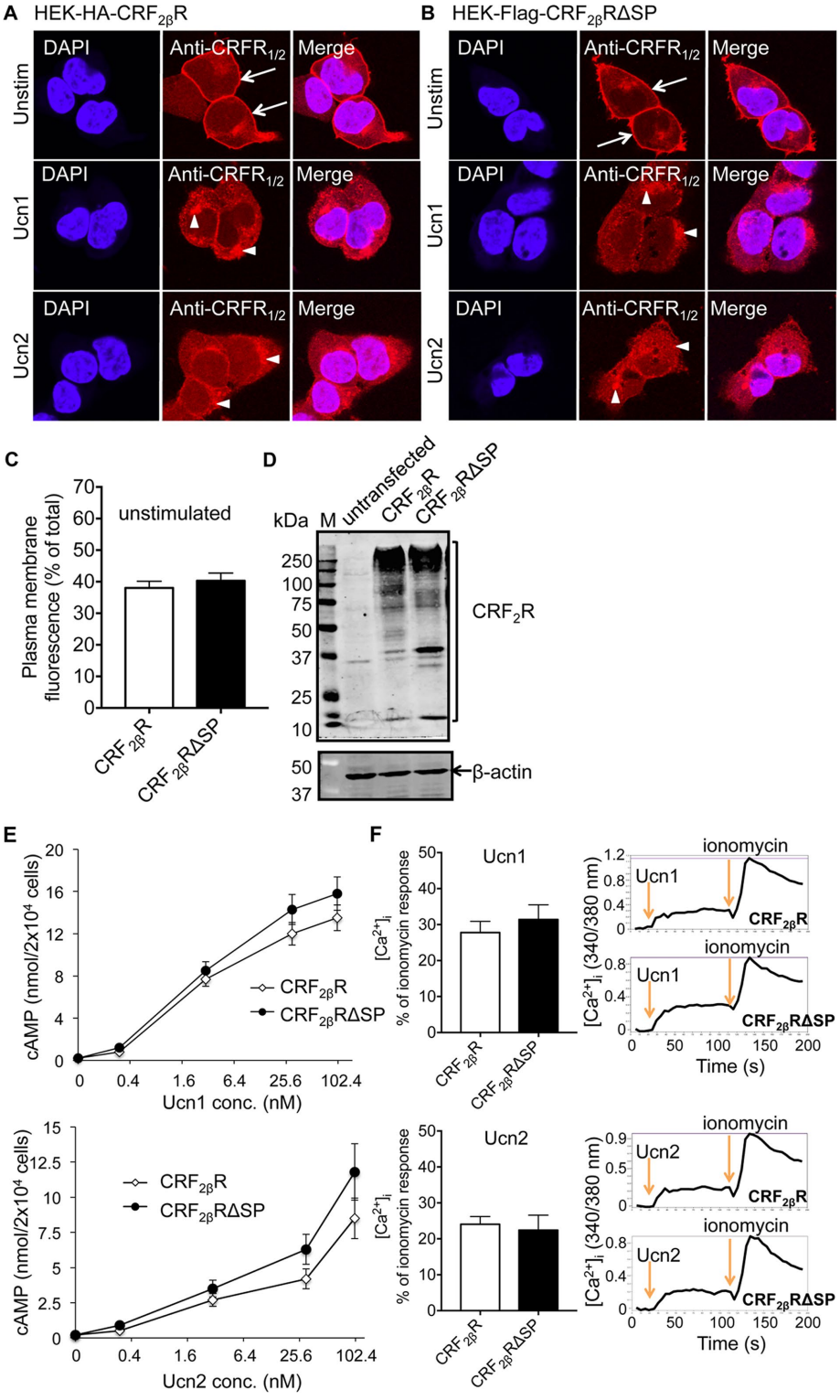

FIGURE 3: Full-length and ΔSP versions of $CRF_2βR$ exhibit similar subcellular localization and downstream cAMP and Ca^{2+} responses. HEK293 cells stably expressing HA-$CRF_2βR$ or Flag-$CRF_2βR$ΔSP were seeded on coverslips and immunostained using anti $CRFR_{1/2}$ antibody. Stimulation with 100 nM of agonists Ucn1 or Ucn2 resulted in internalization (arrowheads) of both full-length (A) and ΔSP (B) versions of $CRF_2βR$s from the cell surface (*arrows*). Representative images are shown ($n = 2$ coverslips per condition, and each experiment was performed three times). Scale bar: 10 μm. (C) Quantification of images in row 1 of A and B. The percentage of total fluorescence at the cell surface for both versions of $CRF_2βR$s was quantified. Cell surface expression was found to be similar between $CRF_2βR$ and $CRF_2βR$ΔSP ($n = 24$ cells for each condition; two-tailed unpaired Student's *t* test: n.s.). (D) Western blot analysis of HEK293 cells expressing HA-$CRF_2βR$ or Flag-$CRF_2βR$ΔSP showed similar receptor expression levels with both constructs. Untransfected cells were used as negative control. (E) cAMP levels increased significantly from baseline values upon stimulation with either Ucn1 or Ucn2 in a dose-dependent manner ($p < 0.05$ vs. baseline values with ligand concentrations >1.6 nM; two-tailed unpaired Student's *t* test, mean ± SEM of three experiments in triplicate) in both full-length and ΔSP versions of $CRF_2βR$s. Importantly, both versions of $CRF_2βR$s showed similar increases in cAMP levels at all doses tested (two-tailed unpaired Student's *t* test: n.s.). (F) Peak $[Ca^{2+}]_i$ increased in response to 100 nM Ucn1 or Ucn2 stimulations in both full-length and ΔSP versions of $CRF_2βR$s to a similar degree (normalized to peak ionomycin responses). Data are mean ± SEM. No significant differences were found between $CRF_2βR$ and $CRF_2βR$ΔSP (two-tailed unpaired Student's *t* test: n.s.). Representative traces of $[Ca^{2+}]_i$ are shown ($n = 3$ wells per condition, and each experiment was performed three times).

C-terminal HA epitope were used. IP of Flag-PAR_2-HA was performed using anti-HA antibodies and separated by SDS–PAGE. While actin was present in all input lanes (Figure 4G), actin did not coimmunoprecipitate with Flag-PAR_2-HA (Figure 4H and Supplemental Figure S1B). Taken together, these data suggest that CRF_1R interacts with $CRF_2βR$ both under unstimulated and various agonist-stimulated conditions and that actin specifically interacts with the CRF receptor complex, further confirming our MS findings.

CRF_1R + $CRF_2βR$ heteromerization alters agonist-induced internalization of CRF_1R

We have previously shown that CRF_1R traffics and internalizes to early endosomes in response to its cognate agonists CRF and Ucn1 (Hasdemir *et al.*, 2012). We determined whether coexpression of $CRF_2βR$ΔSP with CRF_1R alters this trafficking behavior. To study trafficking of receptors exclusively from the cell surface, we labeled the cell-surface receptors by incubating the cells with anti-HA antibody (for HA-CRF_1R) or anti-Flag antibody (for Flag-$CRF_2βR$ΔSP). We have previously demonstrated that surface-tagged CRF_1R trafficked similarly to untagged receptors (Hasdemir *et al.*, 2012), as has been observed with other GPCRs (Hasdemir *et al.*, 2007). Under unstimulated conditions, $CRF_2βR$ΔSP and CRF_1R expressed individually were found at the cell surface (Figure 5, A–C, row 1, and Figure 5, D–G). As expected, CRF stimulation showed modest internalization of $CRF_2βR$ΔSP (Figure 5A, row 2, and D), whereas Ucn2 caused

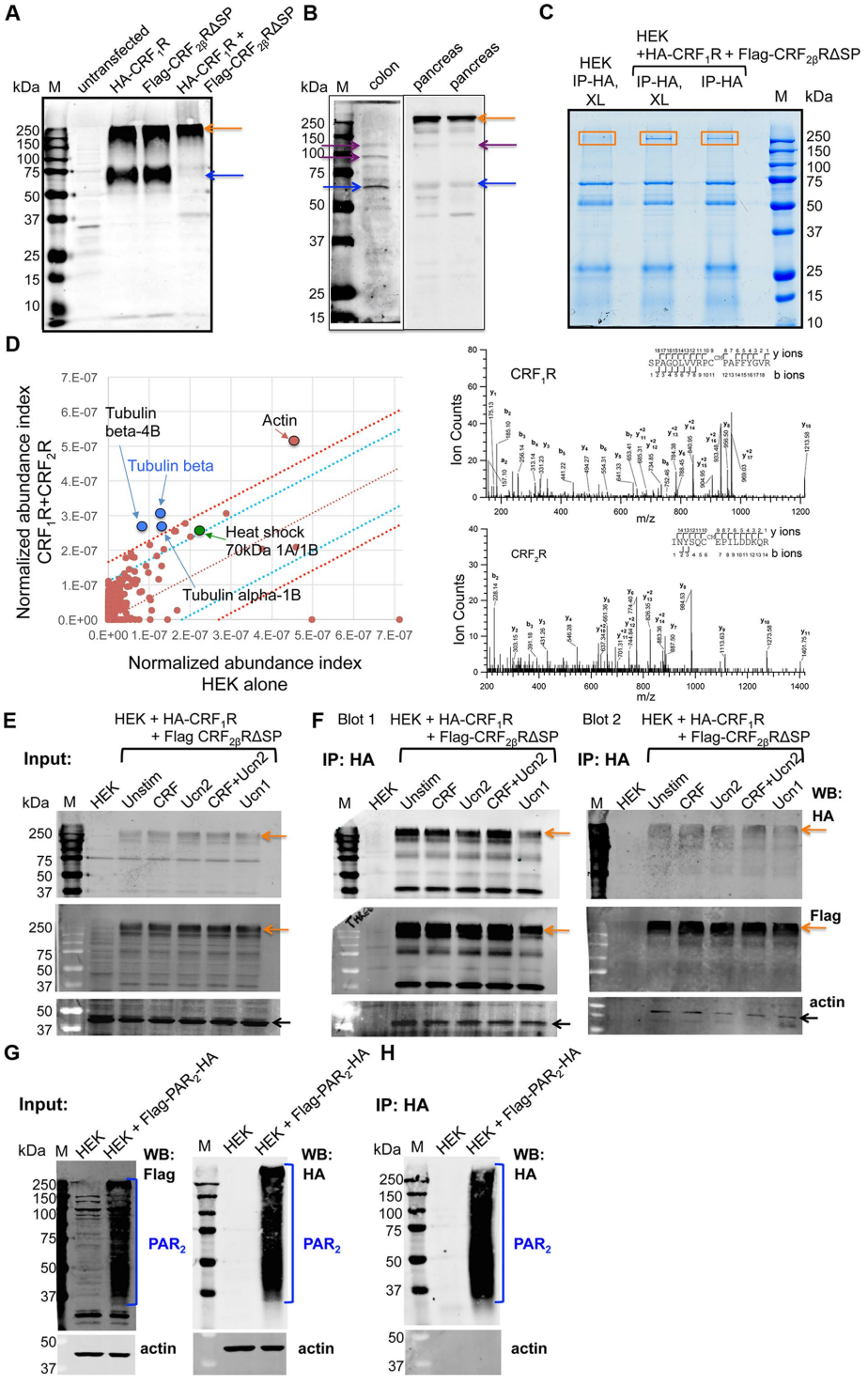

FIGURE 4: CRF_1R and CRF_2R form heteromeric complexes. (A) Western blot analysis of HEK293 showed bands at ~70 kDa and ~250 kDa in cells transfected with either HA-CRF_1R or Flag-$CRF_2\beta R\Delta SP$, whereas only a prominent band at ~250 kDa was seen in cells cotransfected with both HA-CRF_1R+Flag-$CRF_2\beta R\Delta SP$, suggesting heteromerization and formation of a supercomplex. Untransfected cells were used as negative control. (B) Western blot analysis of mouse colon or pancreas whole-tissue lysates using anti-$CRFR_{1/2}$ antibody showed a band at ~60 kDa corresponding to the predicted size of CRFR monomers (blue arrow), as well as bands at ~100 kDa and ~120 kDa, which may represent CRFR dimers (purple arrow). In mouse pancreas, an additional strong band at~250 kDa (orange arrow) was also detected. (C) IPs using anti-HA antibody were performed from cotransfected HA-CRF_1R+Flag-$CRF_2\beta R\Delta SP$ HEK293 cell lysates stimulated with 100 nM CRF for 30 min. Coomassie blue–stained gel of IPs showed a band at ~250 kDa in lysates from cotransfected, but not untransfected, cells (box). These bands were excised and processed for MS. XL, cross-linked; M, marker ($n = 3$–4 for IP and 2–3 for MS). (D) MS analysis of the excised bands revealed that tubulin α/β-chain, actin, and Hsp70 were proteins that were specifically enriched in CRF_1R+$CRF_2\beta$ heteromeric complexes. Scatter plot showing relative enrichment of HA-CRF_1R associated proteins in anti-HA vs. mock pull downs. Intervals of confidence for 95% (blue lines) and 99.7% (red lines) are indicated. Spectral analysis: High-energy collision dissociation–tandem mass spectra obtained from precursor ions with mass 707.7146^{+3} (CRF_1R) and 626.9720^{+3} (CRF_2R) found in tryptic digests of immunoaffinity pull downs of HA-CRF_1R corresponding to peptides spanning residues S58 to R76 of human CRF_1R and I93 to R107 of human CRF_2R. b- and y-type ion series are labeled in the figure. (E, F) Co-IPs and Western blots showing presence of CRFR heteromeric complexes of ~250 kDa size. Anti-HA or anti-Flag antibodies were used in Western blot analyses of HA-CRF_1R+Flag-$CRF_2\beta R\Delta SP$ cotransfected HEK293 cells to detect presence of individual receptor in this complex. Cells were stimulated with various agonists (100 nM) as indicated, and IP was performed using anti-HA antibody. Both the cell lysate inputs (E) and IPs (F) show bands at ~250 kDa in unstimulated and various agonist-stimulated cells. Biological replicates of IPs are shown in F, blots 1 and 2, and Supplemental Figure S1A. The blots were also probed for β-actin, confirming that input had similar levels of total protein and showing that β-actin is coimmunoprecipitated with the CRF receptor complex. Untransfected cells were used as negative control, and no major bands were detected in IP with either anti-HA, anti-Flag, or anti–β-actin antibodies. (G, H) Co-IPs and Western blots showing presence of Flag-PAR_2-HA detected by either HA or Flag antibodies in stably expressing HEK293 cells. Both the cell lysate inputs (G) and IPs (H) show PAR_2 as a characteristic smear from ~250 kDa to ~30 kDa due to various posttranslational modifications. While actin was unequivocally present in the input; actin did not coimmunoprecipitate with Flag-PAR_2-HA or untransfected HEK293 cells that were used as negative control.

more robust internalization (Figure 5A, row 2 vs. row 4, and D; $p < 0.0001$ vs. unstimulated and CRF). As expected, stimulation of cells expressing CRF_1R with CRF resulted in robust receptor internalization, whereas Ucn2 did not (Figure 5B, row 2 vs. row 4, and E; $p < 0.0001$ vs. unstimulated and Ucn2). Ucn1 that exhibits 10-fold higher binding affinity for CRF_2R and CRF_1R in vitro than CRF or Ucn2 (Pal *et al.*, 2010) showed less internalization of $CRF_2\beta R\Delta SP$ than Ucn2 (Figure 5A, row 3, and D; $p < 0.01$ Ucn2 vs. Ucn1). Ucn1 stimulation also resulted in internalization of CRF_1R to a similar degree as CRF (Figure 5B,

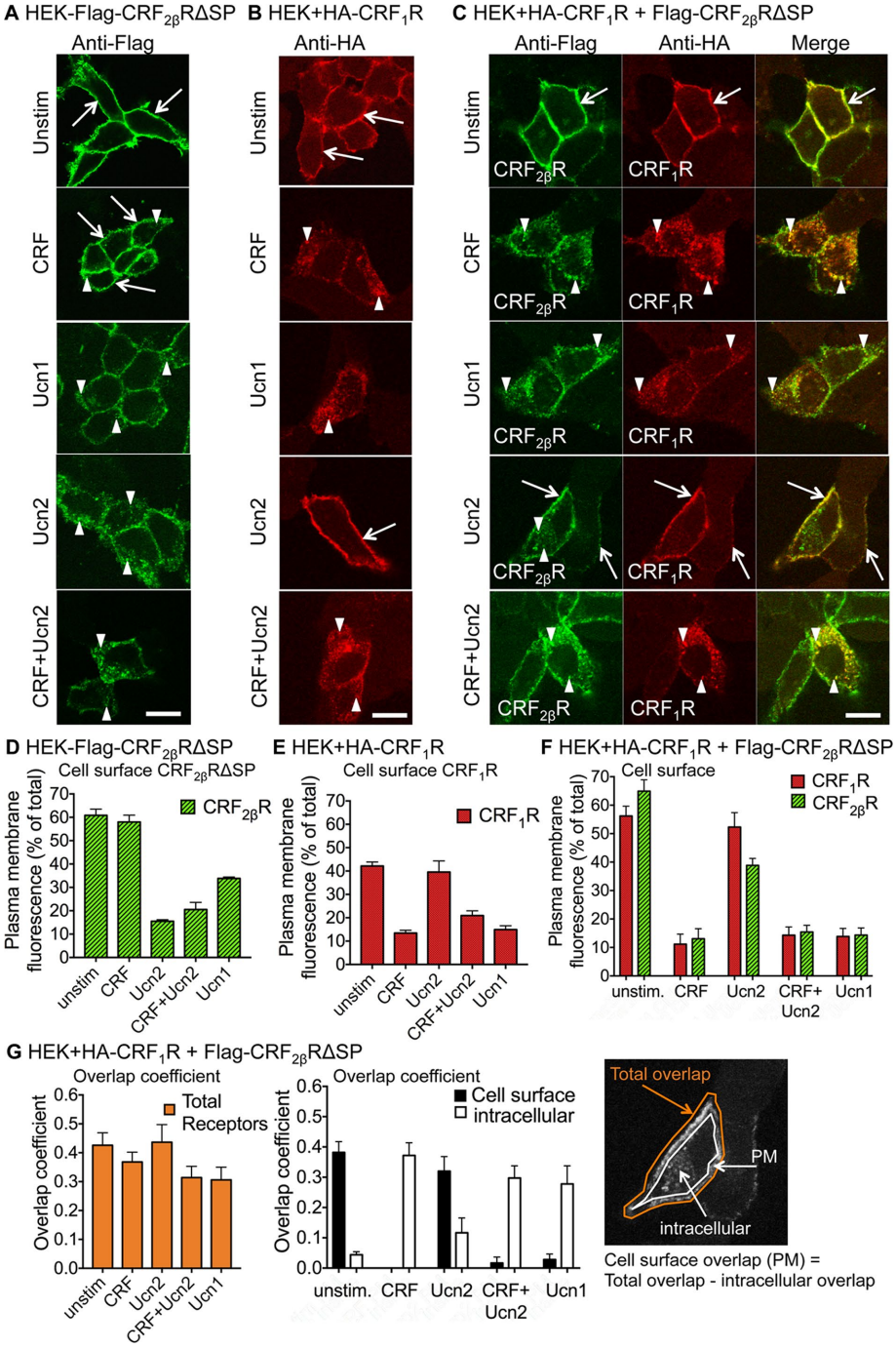

FIGURE 5: CRF_1R+$CRF_2\beta R$ heteromers show altered trafficking upon agonist stimulation. For elucidation of internalization of CRF receptors expressed on the cell surface, HEK293 cells transiently transfected with Flag-$CRF_2\beta R\Delta SP$ or HA-CRF_1R or cotransfected with both CRFRs were incubated with either anti-Flag, anti-HA, or both antibodies together for 45 min, washed, stimulated with buffer (unstimulated control) or different agonists for 30 min, fixed with 4% paraformaldehyde, and immunostained. (A) In cells transfected with Flag-$CRF_2\beta R\Delta SP$ alone, $CRF_2\beta R\Delta SP$ translocated from the plasma membrane to intracellular vesicles upon Ucn1, Ucn2, or CRF+Ucn2 stimulations, but not upon CRF stimulation. (B) In cells transfected with HA-CRF_1R alone, CRF_1R translocated from the plasma membrane to intracellular vesicles after CRF, Ucn1, or CRF+Ucn2 stimulations, but not after Ucn2 stimulation. (C) In cells cotransfected with both HA-CRF_1R+Flag-$CRF_2\beta R\Delta SP$, Ucn1 resulted in cointernalization of both receptors, as expected. CRF also resulted in cointernalization of both receptors (yellow, merge images), whereas Ucn2 stimulation appeared to inhibit internalization of both CRF receptors. Costimulation with CRF+Ucn2 resulted in internalization of both receptors in cells coexpressing both receptors. Representative images are shown ($n = 2$ coverslips per condition, and each experiment was performed three times). Scale bar: 10 μm. Quantification of images of cells transfected with (D) Flag-$CRF_2\beta R\Delta SP$ alone, (E) HA-CRF_1R alone, or (F) cotransfected with both HA-CRF_1R+Flag-$CRF_2\beta R\Delta SP$. The percentage of total fluorescence at the cell surface (plasma membrane) was determined for each receptor under various stimulations or unstimulated conditions ($n = 5$–23 cells per condition). (G) Quantification of overlap coefficient (colocalization) of HA-CRF_1R+Flag-$CRF_2\beta R\Delta SP$ in cotransfected cells under various stimulations or unstimulated conditions (overlap coefficient: 0, no overlap; 1, complete overlap; $n = 5$–12 cells per condition). Example cell illustrates how the regions of interest were drawn for image quantification. Cell surface colocalization values were determined as follows: total overlap expression coefficient – intracellular overlap expression coefficient. One-way ANOVA followed by post hoc Tukey's multiple comparisons were performed for graphs (D–G), and p values are given in the text.

row 3, and E), suggesting that in vitro binding affinities that take only the ligand-binding domain of the receptor into account, may not reflect how the receptor may behave when expressed in its native form. In cells coexpressing CRF_1R+$CRF_2\beta R\Delta SP$, image quantification showed that both CRF receptors were expressed at similar levels at the cell surface (Figure 5F) with little intracellular colocalization (Figure 5G). Both receptors internalized upon CRF stimulation (Figure 5C, panel 3, row 2, and F; $p < 0.0001$ vs. unstimulated) and robust colocalization was evident (Figure 5G). Ucn1 had similar effects and resulted in internalization and colocalization of the two coexpressed receptors in intracellular vesicles (Figure 5C, panel 3, row 3, F, and G; $p < 0.0001$ vs. unstimulated). Ucn2 stimulation resulted in little cointernalization or intracellular colocalization (Figure 5C, panel 3, row 4, F, and G). Upon Ucn2 stimulation, CRF_1R+$CRF_2\beta R\Delta SP$ remained largely localized to the plasma membrane, and only what appeared to be the CRF_1R-dissociated portion of $CRF_2\beta R\Delta SP$ was found to be intracellular (Figure 5F), as was evident by little colocalization of intracellular $CRF_2\beta R\Delta SP$ with CRF_1R (Figure 5C, panel 3, row 4, and Figure 5G). Simultaneous stimulation of the receptor with CRF+Ucn2 resulted in robust internalization and colocalization in the cytoplasm of both receptors (Figure 5C, panel 3, row 5, F, and G; $p < 0.0001$ vs. unstimulated). Importantly, total colocalization coefficient of CRF receptors in unstimulated conditions and upon stimulation with various ligands was similar (Figure 5G). These observations suggest that coexpression of CRF_1R and $CRF_2\beta R\Delta SP$

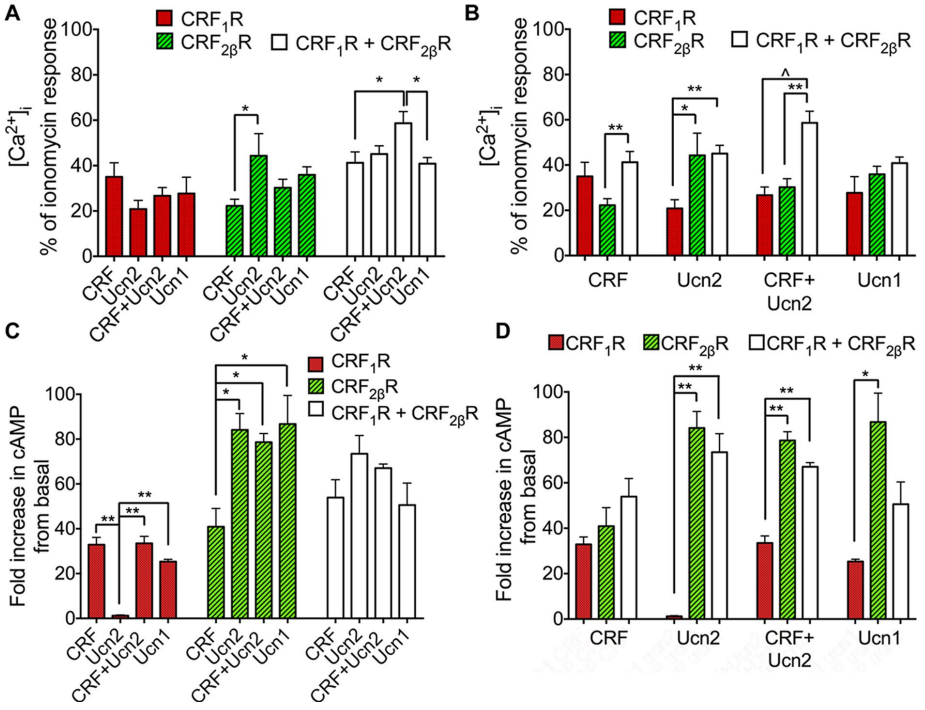

FIGURE 6: CRFR heteromerization alters agonist-mediated calcium and cAMP signaling. Bar graphs showing peak $[Ca^{2+}]$ signals or increase in cAMP levels in HEK293 cells expressing CRF_1R and $CRF_2\beta R\Delta SP$ and coexpressing CRF_1R+$CRF_2\beta R\Delta SP$ in response to various agonist stimulations (100 nM). (A) Stimulation of CRF_1R with all agonists resulted in similar peak Ca^{2+} responses, whereas Ucn2 stimulation of $CRF_2\beta R\Delta SP$ expressing cells resulted in approximately twofold higher peak Ca^{2+} responses. In CRF_1R+$CRF_2\beta R\Delta SP$ coexpressing cells, CRF+Ucn2 stimulation resulted in ~1.5-fold higher peak Ca^{2+} signal compared with stimulation with CRF or Ucn1 alone. (B) After stimulation with CRF, cells coexpressing both CRFRs showed approximately twofold higher peak Ca^{2+} signal compared with cells expressing $CRF_2\beta R\Delta SP$ alone. Ucn2 stimulation resulted in approximately twofold higher peak Ca^{2+} signals in cells coexpressing both CRFRs and $CRF_2\beta R\Delta SP$ alone compared with cells expressing CRF_1R alone. Simultaneous stimulation with CRF+Ucn2 increased peak Ca^{2+} signal by approximately twofold in cells coexpressing both CRFRs compared with cells expressing individual CRFRs, whereas Ucn1, which is known to have equipotent and 10-fold higher binding affinities for both CRFRs, did not significantly alter peak Ca^{2+} signal when both CRF receptors were coexpressed. (C) Unlike the other agonists, stimulation of CRF_1R with Ucn2 did not result in a measurable cAMP response. Ucn2 increased cAMP levels in $CRF_2\beta R\Delta SP$-expressing cells and the levels were approximately twofold greater than those induced by CRF. (D) In contrast to Ca^{2+} signals, cAMP responses to CRF+Ucn2 stimulation were not higher in CRF_1R+$CRF_2\beta R\Delta SP$ coexpressing cells compared with cells expressing $CRF_2\beta R\Delta SP$ alone. Data are mean ± SEM. Significance was calculated by one-way ANOVA Tukey's multiple comparisons tests. *, $p < 0.05$; **, $p < 0.005$; ^, $p < 0.0005$; $n = 3$ wells per condition, and each experiment was performed three times.

forms heteromeric complexes that affect one another's trafficking behavior and cointernalize upon specific agonist stimulations.

CRF_1R+$CRF_2\beta R$ heteromerization alters agonist-mediated intracellular calcium $[Ca^{2+}]_i$ and cAMP signaling

It is well established that CRF binds both CRF_1R and CRF_2R, whereas Ucn2 binds exclusively to CRF_2R (Pal *et al.*, 2010). We tested the notion that binding affinities might not be directly proportional to receptor function. In HEK293 cells expressing CRF_1R alone, stimulation with individual agonists or in combination evoked Ca^{2+} responses to a similar degree (Figure 6, A and B), whereas Ucn2 stimulation did not result in a measurable cAMP response (Figure 6, C and D). In HEK293 cells expressing $CRF_2\beta R\Delta SP$ alone, Ucn2 stimulation evoked Ca^{2+} responses and induced cAMP levels that were approximately twofold greater than those induced by CRF (Figure 6, A–D). Next we determined whether CRF receptor heteromerization alters the coexpressed receptors' Ca^{2+} or cAMP signaling capabilities as opposed to individually expressed CRF_1R and $CRF_2\beta R$. Ca^{2+} responses of cells coexpressing CRF_1R+$CRF_2\beta R\Delta SP$ challenged by CRF+Ucn2 simultaneously were significantly higher than those induced by CRF, Ucn2, or Ucn1 individually (Figure 6, A and B). When cells coexpressing CRF_1R+$CRF_2\beta R\Delta SP$ were simultaneously stimulated with CRF+Ucn2, the peak Ca^{2+} signal showed an additive effect compared with individually expressing receptors (Figure 6B). In contrast to Ca^{2+} levels, cAMP levels were similarly increased after stimulation with individual agonists or simultaneous stimulation with CRF+Ucn2 (Figure 6, C and D). Thus, while CRF_1R+$CRF_2\beta R\Delta SP$ internalize together as heteromers in response to a single agonist, activation and downstream coupling with G proteins of both receptors after stimulation with their cognate agonists may be necessary for functional efficacy. We reasoned that Ucn1 that binds both CRF_1R and $CRF_2\beta R$ with equal, but 10-fold higher affinities than either CRF or Ucn2 (Pal *et al.*, 2010) would induce synergistic cooperation of CRFR heteromers and secondary messenger signaling. However, contrary to our prediction, stimulation of cells expressing CRF_1R+$CRF_2\beta R\Delta SP$ with Ucn1 did not result in significantly different Ca^{2+} responses than those observed in cells expressing individual CRFRs (Figure 6B), whereas cAMP levels in coexpressing cells were in between those expressing CRF_1R or $CRF_2\beta R\Delta SP$ alone (Figure 6D). This suggests that activation of the receptor heteromers by Ucn1 was insufficient to induce synergistic cooperation.

Coexpression of $CRF_2\beta R$ switches CRF_1R trafficking and signaling from an actin-independent to an actin-dependent pathway

Receptor-mediated endocytosis can occur using the actin cytoskeleton (Lamaze *et al.*, 1997). Mass spectrometry analysis of CRF_1R+$CRF_2\beta R$ multimeric complex revealed actin as an interacting partner that coimmunoprecipitated with CRF_1R (Figure 4, D–F). We investigated whether individually expressed CRF receptors and/or CRF_1R+$CRF_2\beta R\Delta SP$ heteromers require polymerization of actin to translocate from the ER–Golgi complex to the cell surface and vice versa. HEK293 cells expressing only CRF_1R continued to show cell surface receptor expression even after treatment of cells with cytochalasin D, which inhibits actin polymerization and causes aggregation of actin filaments on endosomes (Figure 7A, phalloidin red stains F-actin). Cytochalasin D treatment led to significant accumulation of $CRF_2\beta R\Delta SP$ in intracellular vesicles that showed strong colocalization with phalloidin (Figure 7A, bottom panel), indicating that trafficking and subcellular localization of $CRF_2\beta R\Delta SP$ was disrupted by inhibiting actin polymerization. Importantly, when CRF_1R+$CRF_2\beta R\Delta SP$ were coexpressed, treatment with cytochalasin D resulted in both CRF receptors being trapped in F-actin

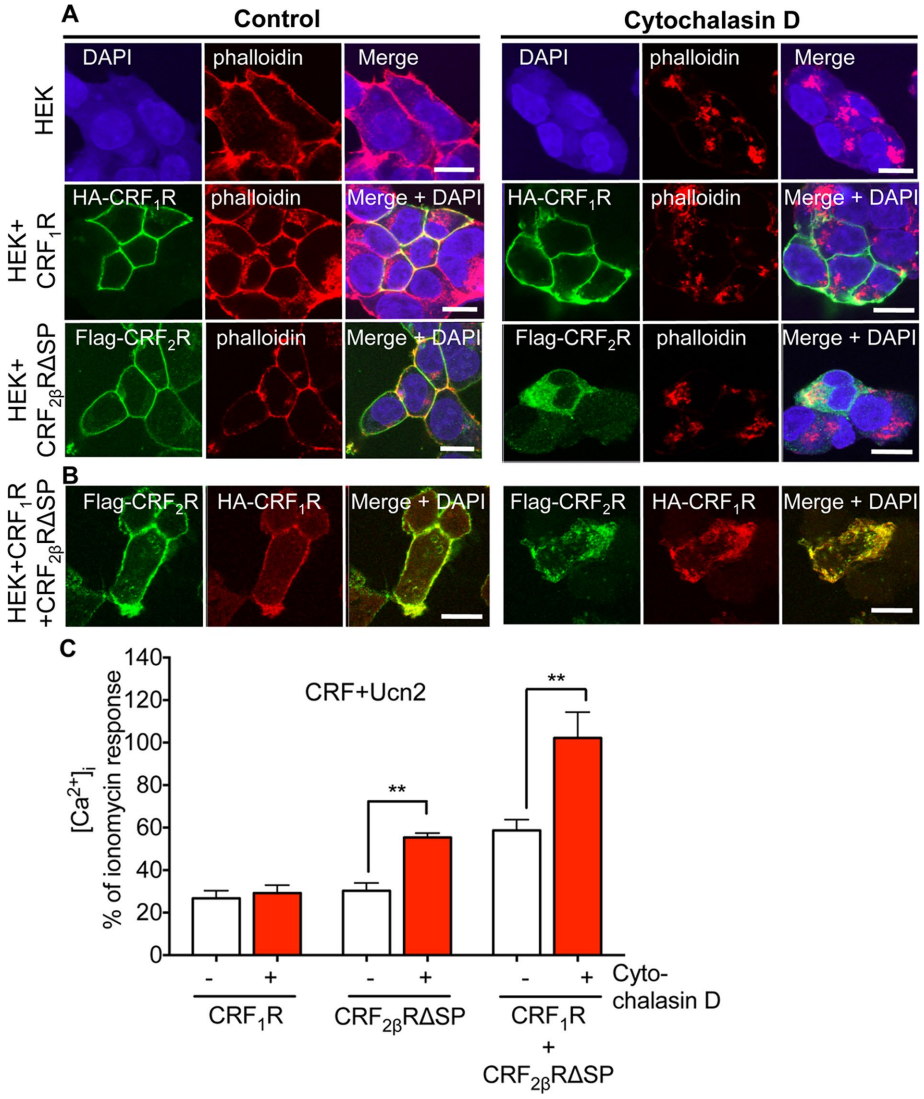

FIGURE 7: Coexpression of $CRF_2\beta R$ switches CRF_1R trafficking from actin-independent to actin-dependent. (A) Treatment of HEK293 cells with cytochalasin D, an inhibitor of F-actin polymerization resulted in aggregation of F-actin filaments (stained with phalloidin-red, top panel). CRF_1R continued to show cell surface expression (middle panel), whereas $CRF_2\beta R\Delta SP$ colocalized with F-actin aggregates (bottom panel) after cytochalasin D treatment. (B) In HA-CRF_1R+Flag-$CRF_2\beta R\Delta SP$ coexpressing cells, cytochalasin D treatment resulted in both receptors being trapped in aggregates, suggesting that trafficking of CRFR heteromers is F-actin dependent. Scale bar: 10 µm. Representative images are shown ($n = 2$ coverslips per condition, and each experiment was performed three times). (C) Ca^{2+} signals in response to CRF+Ucn2 stimulation. Bar graphs showing increased peak Ca^{2+} signals in $CRF_2\beta R\Delta SP$ and CRF_1R+$CRF_2\beta R\Delta SP$ coexpressing cells, but not in CRF_1R HEK293 cells after pretreatment with cytochalasin D, as compared with buffer treatment. Data are mean ± SEM. Significance was calculated by the two-tailed unpaired Student's *t* test. **, $p < 0.005$; $n = 3$ wells per condition, and each experiment was performed three times.

aggregates (Figure 7B), indicating that the fate of CRF_1R depends on formation of heteromeric complexes with $CRF_2\beta R\Delta SP$ that alter trafficking of CRF_1R from an actin-independent to an actin-dependent pathway.

Destabilization of actin cytoskeleton in polarized Caco2 cells inhibits receptor-mediated endocytosis at the apical but not the basolateral surface (Gottlieb *et al.*, 1993). Polymerization of actin filaments controls formation of clathrin-coated vesicles in a context-dependent manner (Boulant *et al.*, 2011). We investigated the role of the actin cytoskeleton in mediating Ca^{2+} signaling. We stimulated HEK293 cells expressing individual CRFRs or coexpressing both receptors with CRF+Ucn2 in the presence or absence of cytochalasin D (Figure 7C). Ca^{2+} responses in cells expressing CRF_1R were not affected by cytochalasin D treatment, further confirming our observation that trafficking of CRF_1R to the cell surface from an intracellular locale does not require presence of intact actin filaments. However, Ca^{2+} responses in cells expressing $CRF_2\beta R\Delta SP$ alone or coexpressing both CRF_1R+$CRF_2\beta R\Delta SP$ were significantly affected by cytochalasin D incubation (Figure 7C). Treatment of cells with cytochalasin D increased Ca^{2+} responses by 40–50%. The additive effect of simultaneous stimulation with CRF+Ucn2 was maintained in the presence of cytochalasin D (Figure 7C). This indicated that disruption of actin polymerization specifically affected Ca^{2+} signaling mediated by $CRF_2\beta$ when expressed alone and also heteromeric complexes that contain $CRF_2\beta R$. Thus actin dependence of heteromeric CRFR signaling possibly requires dual and simultaneous receptor stimulation with specific agonists.

DISCUSSION

CRF_1R and CRF_2R receptor signaling pathways are being explored as potential drug targets for a plethora of disorders, ranging from anxiety and depression to obesity (Doyon *et al.*, 2004; Henckens *et al.*, 2016). In this study, we made several novel observations. First, we show that $CRF_2\beta R$ harbors a cleavable SP in its N-terminal. Second, agonist-binding affinities as defined by in vitro assays do not translate to functional potencies. For example, both CRF and Ucn2 are known to have equal binding affinities for CRF_2R, but here we show that Ucn2 stimulation results in approximately twofold higher cAMP/Ca^{2+} signaling than CRF. Third, we show that CRF_1R and CRF_2R interact with other regulatory proteins to form multimeric complexes. These high-mobility complexes were also seen in vivo in pancreatic tissue. Interaction of CRF_1R and CRF_2R was confirmed by co-IP and MS. Fourth, interaction of CRF_1R with CRF_2R resulted in cointernalization of both receptors after stimulation with CRF, but not Ucn2 and altered downstream intracellular Ca^{2+} signaling. Finally, we show that trafficking of CRF_2R, but not CRF_1R, is actin dependent. Coexpression of both CRF_1R and CRF_2R results in altering trafficking fate of CRF_1R from actin independent to actin dependent.

CRF_1R is shown to have a cleavable SP, whereas $CRF_2\alpha R$ harbors a pseudo-SP (Teichmann *et al.*, 2012). Deletion of the putative SP of $CRF_2\alpha R$ prevents the receptor from exiting the ER (Rutz *et al.*, 2006). Here we show that not only does $CRF_2\beta R$ harbor a cleavable SP, but it is also functional without its N-terminal SP. The pseudo-SP of

$CRF_2\alpha R$ is thought to prevent oligomerization (Teichmann *et al.*, 2012); in contrast, $CRF_2\beta R$ without its SP is able to form heteromers with CRF_1R or homomers. CRF_1R is shown to exist as a monomer or dimer (Teichmann *et al.*, 2014), and our data from pancreas, colon, and transfected HEK293 cells shows that $CRF_2\beta R$ can also exist as monomer or dimer.

We observed that in vitro binding affinities of agonists Ucn1 and Ucn2 with CRF_2R do not necessary translate to trafficking and cAMP and/or Ca^{2+} signaling properties. Ucn1 is known to exhibit a 10-fold higher binding affinity to both CRF_1R and CRF_2R than CRF or Ucn2, whereas Ucn2 is known to bind only to CRF_2R (Vaughan *et al.*, 1995; Lewis *et al.*, 2001; Reyes *et al.*, 2001). Here we found that Ucn2 stimulation evoked Ca^{2+} and cAMP responses that were similar in magnitude to those seen with Ucn1 in cells expressing $CRF_2\beta R$. All three agonists (CRF, Ucn1, and Ucn2) evoked similar Ca^{2+} responses in cells expressing CRF_1R alone, whereas Ucn2 did not increase intracellular cAMP levels in cells expressing CRF_1R. CRF, Ucn2, and a combination of both agonists significantly increased peak Ca^{2+} responses in cells coexpressing both receptors compared with cells expressing individual CRF receptors. This is in contrast to Ucn1 stimulation, where no such differences were seen, despite Ucn1 exhibiting higher affinity for $CRF_2\beta R$. This is in agreement with published data that showed Ucn1 stimulation caused CRF_1R to traffic through a slower recycling Rab11 pathway (Hasdemir *et al.*, 2012). Ucn2 increased cAMP levels in cells coexpressing both receptors, whereas Ucn1 dampened the effect. Surprisingly, despite Ucn1 exhibiting equal binding affinities for both receptors, levels of cAMP in $CRF_2\beta R$-expressing cells were twofold higher than CRF_1R-expressing cells. Interestingly, stimulation of coexpressed CRF receptors with Ucn3, another CRF_2R-specific agonist was shown to decrease Ca^{2+} responses (Mahajan *et al.*, 2014). Taken together, these data strongly suggest that in vitro binding affinities determined using ligand-binding domains of receptors may not be reflective of in vivo affinities or function. Intracellular cAMP and Ca^{2+} signaling regulates many downstream cellular functions, including changes in phosphorylation levels of various MAPK, including ERK1/2. Previous coexpression studies of CRF_1R and $CRF_2\beta R$ in HEK293 cells showed that CRF_1R did not alter Ucn2-induced activation of cAMP, p38, or p42/p44 MAPK (Markovic *et al.*, 2008). Furthermore, heteromerization of the two CRF receptors might allow CRF_2R-specific agonists such as Ucn2 and Ucn3 to regulate functions that are driven by the CRF_1R or allow for nuanced signaling by high-affinity agonists, such as Ucn1. However, the exact nature of this interaction and consequences of preventing CRFR heteromerization require further investigation.

Previous studies have suggested CRF receptor cross-talk (Mahajan *et al.*, 2014); however, the physical heteromeric interaction of CRF receptors or association with ancillary proteins has not been demonstrated. Drugs that antagonize one specific CRFR may have unintended consequences on CRFR function in cells that coexpress both CRFRs. Here we show that CRF_1R and $CRF_2\beta R$ interact and form heteromers in a multimeric complex with ancillary proteins that include cytoskeletal proteins. Trafficking and signaling of heteromeric CRFRs is distinct from mono- or homomers and so is their dependence on the actin cytoskeleton (model proposed in Figure 8). The concept of GPCR heteromerization was first introduced by Rodbell, who showed that GPCRs were not simple monomeric structures but formed large complexes with G proteins and adenylyl cyclase (Rodbell, 1995). The functional significance of GPCR heteromerizations remains an area not well understood but is emerging to be of considerable pathophysiological importance. For example, heteromerization of GABAbR1 and GABAbR2 within the ER is

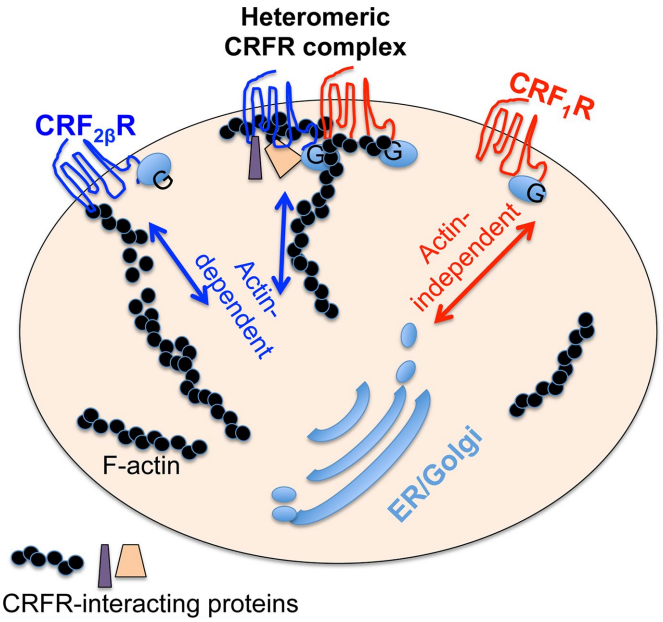

FIGURE 8: Proposed model for CRFR heteromerization interaction with ancillary proteins in a supercomplex. Schematic diagram shows a simplified view of CRF receptors trafficking from the endomembrane system to the plasma membrane and vice versa. CRF_1R traffics to and from the endomembrane system to the cell surface in an actin-independent manner, whereas $CRF_2\beta R$ uses an actin-dependent path to traffic to and from the cell surface. Heteromerization of CRF_1R+CRF_2R changes the fate of CRF_1R from an actin-independent to an actin-dependent trafficking pathway. CRFR heteromers interact with ancillary proteins, such as Hsp70, tubulin, and actin.

necessary for adequate GABAbR1 expression on the cell surface (Margeta-Mitrovic *et al.*, 2000). The serotonin receptor $5\text{-}HT_{2A/C}R$ and vasopressin receptor V1B interact with CRF_1R to increase anxiety-like behavior in rats (Magalhaes *et al.*, 2010) or modulate CRF function (Murat *et al.*, 2012), respectively.

Several cytoskeleton-associated proteins, including F-actin and filamin A, interact with the i3 loop of GPCRs (Binda *et al.*, 2002; Cornea-Hebert *et al.*, 2002; Kim *et al.*, 2002), and this study identified actin, F-actin capping protein, and tubulin as protein partners that associate with the CRF_1R+$CRF_2\beta R$ heteromeric complex. It is possible that the interaction with actin is not "static" but rather an agonist-regulated dynamic process. Based on in vitro individual receptor binding studies, it has been rationalized that Ucn2 and Ucn3 exert their effects via CRF_2R alone, whereas CRF and Ucn1 bind and activate both CRF_1R and CRF_2R (Pal *et al.*, 2010). This might have important therapeutic implications, because Ucn2 is implicated in the pathophysiology of congestive heart failure and type 2 diabetes (Lai *et al.*, 2015). Studies have shown that CRF_1R is the principal receptor involved in stress-adaptive responses, whereas CRF_2R functions to dampen the activity of CRF_1R and ameliorate stress behavior (Hotta *et al.*, 1999; Reyes *et al.*, 2001).

Upon agonist binding, association of CRF receptors with ancillary proteins such as β-arrestins, clathrins, dynamins, and cytoskeleton proteins is essential for proper trafficking and localization of these receptors in specific microdomains. Destabilization of actin cytoskeleton in polarized Caco2 cells inhibits receptor-mediated endocytosis at the apical but not the basolateral surface (Gottlieb *et al.*, 1993). Polymerization of actin filaments controls formation of clathrin-coated vesicles in a context-dependent manner (Boulant *et al.*, 2011). Thus our finding that CRFR heteromers associate

with actin cytoskeleton to mediate trafficking in a agonist-dependent manner is of interest, because stress conditions and drugs that compromise polarization of cytoskeleton proteins may also indirectly affect agonist-receptor signaling at the membrane. Our findings of CRF receptor heteromerization and formation of a multimeric complex that signals in an agonist-dependent manner identify a novel regulatory mechanism of potential relevance for compound pharmacology, because antagonists and drugs that target one CRF receptor only can alter function and signaling of interacting CRF receptors, resulting in off-target side effects.

Migrating and invading carcinoma cells use F-actin–based protrusions to promote trafficking of integrin α/β heteromeric receptors (Paul *et al.*, 2015). F-actin remodeling in pancreatic islet cells is induced by glucose, similar to that seen with cytochalasin D (Kalwat and Thurmond, 2013), and Ucn2 acting via CRF receptors regulates glucose levels in pancreas (Gao *et al.*, 2016). Thus trafficking of CRF receptors, specifically that of CRF_2R, may be of significance in pathophysiological conditions such as diabetes and metabolic diseases. The physiological relevance of our observations is further validated by other studies that showed colocalization between the endogenous CRFRs and actin stress fibers in native uterine smooth muscle cells (Markovic *et al.*, 2007). The subapical actin cytoskeleton is pivotal in regulating fusion and/or fission of zymogen granule membranes with the luminal plasma lemma in the acinar cells, and its redistribution is a crucial event responsible for inhibition of Ca^{2+}-mediated secretion (Singh *et al.*, 2001). Inhibition of actin filament polymerization resulted in $CRF_2\beta R$ being trapped in F-actin aggregates, whereas CRF_1R continued to traffic to the cell surface, suggesting that individually expressed CRF_1R traffics to and from the ER–Golgi to the cell surface in an actin-independent manner (Figure 8). When CRF_1R+$CRF_2\beta R$ were coexpressed, inhibition of actin polymerization prevented normal trafficking of CRF_1R; both receptors colocalized with actin aggregates (Figure 8). Our findings suggest that $CRF_2\beta R$ traffics via an actin-dependent path and alters the fate of CRF_1R trafficking, which may help mediate Ca^{2+} signaling in discrete intracellular regions; however, the precise mechanism remains to be elucidated.

MATERIALS AND METHODS

Materials

Plasmid and reagents were from the following sources: pcDNA-FRT-5.0 plasmid and Fura-2AM (ThermoFisher Scientific); Lipofectamine 2000 (Invitrogen); CRF and urocortins (American Peptide); trypsin (Gold, Mass Spectrometry Grade; Promega); solvents for in-gel digestion, UPLC, water, acetonitrile, and formic acid (HPLC grade; Fisher Scientific); ionomycin (Life technologies); cytochalasin D (Enzo Life Sciences); Alexa Fluor 555 phalloidin red (Cell Signaling).

Primary antibodies were from the following sources: rabbit anti-HA11, rabbit anti-Flag, mouse anti-Flag, mouse anti–β-actin and rabbit anti-actin (Sigma); rat anti-HA11 (Roche); goat anti-$CRFR_{1/2}$ (Santa Cruz Biotechnology). Secondary antibodies were from the following sources: anti-goat, anti-rabbit, anti-rat immunoglobulin G (IgG) coupled to fluorescein isothiocyanate or Rhodamine Red-X (Jackson ImmunoResearch Laboratories); anti-mouse or anti-rat or anti-rabbit IgG coupled to Alexa Fluor 680 (Invitrogen), and coupled to IRDye 800 (Rockland Immunochemicals).

cDNA Constructs

HA-CRF_1R cDNA plasmid was previously cloned and described by us (Hasdemir *et al.*, 2012). A full-length $CRF_2\beta R$ cDNA plasmid previously cloned and described by us (Grammatopoulos *et al.*, 2000; Hasdemir *et al.*, 2012) was used as a template to make $CRF_2\beta R$ constructs: HA-$CRF_2\beta R$ and Flag-$CRF_2\beta R\Delta SP$ in pcDNA-FRT-5.0 vector. Forward primer for HA-$CRF_2\beta R$: 5′GCAGTCTAAGCTTGCCACC*ATG* TACCCATACGATGTTCCAGATTACGCTATGAGGGGTCCCTCAGG3′ (*Hin*dIII site: AAGCTT, Kozak sequence: GCCACC, start site: ATG, HA-Tag: TACCCATACGATGTTCCAGATTACGCT, $hCRF_2R$ sequence: ATGAGGGGTCCCTCAGG). Reverse primer: 5′CGCAGATCTCGAGTCACACAGCGGCCGTCTGCTTGATGCTG3′ (*Xho*I site: CTCGAG, stop codon: TGA, $hCRFR_2$ sequence: CAAGCAGACGGCCGCTGTG). Flag-$CRF_2\beta R$: Flag-tagged full-length $CRF_2\beta R$ was cloned in pCMV-Tag 1 vector (Agilent Technologies) in *Bgl*II and *Xho*I restriction sites in the multiple cloning sequence: forward primer: 5′CAAGATCTTAATGAGGGGTCCCTCAGGGCC3′; reverse primer: 5′TGCTCGAGCACAGCGGCCGTCTGCTTG3′ (Figure 2B). However, while the receptor expression was robust from both the HA- and Flag-tagged constructs as determined using the C-terminal antibody, the Flag tag was not detected, whereas the HA tag was seen in intracellular vesicles (Figure 2C). Thus it was concluded that the N-terminal sequence of the receptor is cleaved, irrespective of the tag.

We next made a Flag-tagged construct that lacked the putative SP sequence (first 26 amino acids) referred to as delta SP (ΔSP) CRF_2R. Flag-tagged 27-461-$CRF_2\beta R$ (Flag-$CRF_2\beta R\Delta SP$) was amplified using Forward primer for Flag-$CRF_2\beta R\Delta SP$: 5′AAGCTTGCCACCATGGACTACAAGGACGACGACGACAAGCCGCTCCAATACGCAGCCG3′ [*Hin*dIII site: AAGCTT, Kozak sequence: GCCACC, start site: *ATG*, Flag-Tag: GACTACAAGGACGACGACGACAAG, $hCRF_2R$ sequence: CCGCTCCAATACGCAGCCG]. Reverse primer: 5′CTCGAG TCACACAGCGGCCGTCTGCTTG3′ [*Xho*I restriction site: CTCGAG, stop codon: *TGA*, $hCRFR_2$ sequence: CAAGCAGACGGCCGCTGTG]. High-fidelity Taq polymerase was used for PCR amplification. Amplified cDNAs were cloned into the *Hin*dIII and *Xho*I within the multiple cloning site of pcDNA-FRT-5.0 vector and sequenced to confirm no additional mutations or mismatches were present before use in transfection and expression studies.

Transfections and generation of stable cell lines

Human embryonic kidney 293 (HEK) cells were grown in DMEM containing 10% heat-inactivated fetal bovine serum in 95% air and 5% CO_2 at 37°C and used up to passage 6. HEK-FLP cells stably expressing HA-$CRF_2\beta R$ or Flag-$CRF_2\beta R\Delta SP$ were generated as described previously for HA-CRF_1R (Hasdemir *et al.*, 2012). In specified experiments, HEK cells were transiently transfected using Lipofectamine 2000 according to the manufacturer's guidelines. Cells were plated 48 h before experiments and incubated in DMEM, 0.1% bovine serum albumin (BSA) for treatments. HEK-FLP cells stably expressing PAR_2 with an N-terminal Flag epitope and a C-terminal HA epitope described previously (Hasdemir *et al.*, 2007) were used as controls for the co-IP experiments.

Immunofluorescence, confocal microscopy, and image analysis

HEK293 cells were seeded on poly-D-lysine (100 µg/ml)-coated coverslips in six-well plates at ~3×10^5 per well. At 48 h posttransfection, cells were processed for immunofluorescence staining either by conventional immunofluorescence method or antibody-tagged receptor method to examine trafficking of receptors exclusively from the plasma membrane. For conventional immunofluorescence staining, cells were incubated with agonists (or not) as indicated. All agonists were applied at 100 nM and included CRF, Ucn1, Ucn2, or fluorescently labeled agonists: 5-carboxyfluorescein-labeled Ucn1 (5-FAM-Ucn1) and Rhodamine Red–labeled CRF (Rhod-CRF). Cells

were washed with phosphate-buffered saline (PBS), fixed with 4% paraformaldehyde (20 min, 4°C), washed, and incubated with blocking buffer containing 0.1% saponin and 1% heat-inactivated normal goat or horse serum for 60 min. Receptors were localized using the primary antibodies (anti-HA, anti-Flag, or anti-$CRFR_{1/2}$; 1:500, 2 h room temperature) and washed and incubated with secondary antibodies conjugated to fluorescein isothiocyanate (FITC) or Rhodamine Red-X (RRX) (1:200, 1 h room temperature) as previously described by us (Hasdemir *et al.*, 2012). For staining of actin filaments, cells were incubated with Alexa Fluor 555 phalloidin red (1:20, 30 min room temperature) after the secondary antibody incubation and then washed before mounting. For studying trafficking of receptors expressed on the cell surface, an antibody-tagged receptor staining protocol was used. Briefly, cells expressing either HA-CRF_1R or Flag-$CRF_2\beta R\Delta SP$ or coexpressing both receptors were incubated with rat anti-HA and/or rabbit anti-Flag (1:100, 45 min at 37°C). Cells were washed and stimulated with 100 nM of CRF, Ucn2, Ucn1, or CRF+Ucn2 for 2 and 30 min or with buffer (unstimulated controls). Cells were fixed, washed, incubated in blocking buffer for 1 h; this was followed by incubation with secondary antibodies conjugated to FITC or RRX (1:200, 1 h room temperature). Cells were imaged with a Zeiss confocal microscope (LSM Meta 510; Carl Zeiss, Thornwood, NY) using a Fluor Plan-Apochromat 63× oil-immersion objective (NA 1.4). Images were collected and simultaneously processed (colored and merged) using the Zeiss (LSM 510) software.

Confocal images were analyzed using Zeiss LSM 510 software. Cell surface expression was quantified by drawing regions of interest on the outside and the inside of the plasma membrane (as illustrated in Figure 5G), which allowed determination of the percentage of total cellular fluorescence at the plasma membrane, as previously described (O'Callaghan *et al.*, 2003; Hasdemir *et al.*, 2007). Colocalization of RRX-stained HA-CRF_1R (red) and FITC-stained Flag-$CRF_2\beta R\Delta SP$ (green) was quantified by measuring the overlap coefficient, with a coefficient of 0 indicating no colocalization and of 1 indicating complete colocalization within the regions of interest as illustrated in Figure 5G.

Receptor Co-IP

HA-CRF_1R and Flag-$CRF_2\beta R\Delta SP$ were cotransfected in HEK293 cells in 10 cm dishes (at ~1×10^6 cells per dish) using Lipofectamine 2000 (Invitrogen). Untransfected HEK-FLP cells and HEK-FLP cells stably expressing Flag-PAR_2-HA were used as additional controls. At 48 h posttransfection, cells were either vehicle treated or stimulated for 30 min with 100 nM of CRF, Ucn2, Ucn1, or CRF+Ucn2 together. IP was performed from both formaldehyde cross-linked cells or non–cross-linked cells with both anti-HA and anti-Flag antibodies. Subsequently, the cells were washed twice with ice-cold PBS and lysed in 500 µl RIPA buffer (50 mM Tris/HCl, pH 7.4, 150 mM NaCl, 5 mM $MgCl_2$, 1 mM EGTA, 10 mM NaF, 10 mM $Na_4P_2O_7$, 0.1 mM Na_3VO_4, 0.5% Nonidet P-40; supplemented with protease inhibitor cocktail [Roche] and phosphatase inhibitor cocktails). Twenty microliters per lysate was used as "IP input," and the rest of the lysate was used for IP. Briefly, each lysate was incubated with 2.5 µg rat anti–HA-antibody in 500 µl RIPA buffer on a rotor overnight at 4°C. Then 30 µl of washed protein A beads (Santa Cruz) was added and incubated on a rotor for 1–2 h at 4°C. The slurry was centrifuged at 3000 rpm for 5 min, and the supernatant was discarded. The beads were washed three times with 1 ml RIPA buffer. Then 30 µl of SDS-sample dye was added, samples were boiled, and IPs were resolved on a 10% SDS–PAGE followed by Western blotting with anti-HA, anti-Flag, and anti–β-actin or anti-actin antibodies.

Western blot analysis

Cells were lysed in RIPA buffer as described above. Lysates (30 µg of protein) or IP samples were boiled with SDS-sample loading buffer, resolved with 10% SDS–PAGE, transferred to polyvinylidene difluoride membranes (Immobilon-FL; Millipore, Billerica, MA), blocked for 1 h, and incubated with anti–β-actin or anti-actin (1:5000), anti-HA (1:1000), anti-Flag (1:1000), or anti-CRFR1/2 (1:1000) (2 h at room temperature). Membranes were incubated with secondary antibodies conjugated to Alexa Fluor 680 or IRDye 800 (1:20,000, 1 h at room temperature), and blots were analyzed with the Odyssey Infrared Imaging System (Li-Cor Biosciences, Lincoln, NE).

Mass spectrometry: reverse-phase LC–MS/MS and data analysis

HA-CRF_1R and Flag-$CRF_2\beta R\Delta SP$ were cotransfected in HEK293 cells, and co-IP was performed as described above. Proteins bound to beads were eluted using 0.2 M glycine (pH 2.0) and neutralized with 1 M Tris-HCl (pH 8.0), and resolved on a 10% SDS–PAGE. In-gel digestion of proteins with trypsin was performed as described previously (Rosenfeld *et al.*, 1992). Peptides were analyzed in an Orbitrap XL (Thermo), in positive ion mode and in information-dependent acquisition mode to automatically switch between MS and MS/MS acquisition. For each MS spectrum, the six most intense multiply charged ions (charge 2–5) over a threshold of 1000 counts were selected for generation of collision-induced dissociation mass spectra. A dynamic exclusion window was applied that prevented the same *m/z* from being selected for 1 min after its acquisition. Peak lists were generated using PAVA software (Guan *et al.*, 2011). The peak lists were searched against the human subset of the SwissProt database using Protein Prospector version 5.2.2. A randomized version of all entries was concatenated to the database to estimate false discovery rates in the searches. Peptide tolerance in searches was 20 ppm for precursor ions and 0.8 Da for product ions, respectively. Peptides containing two miscleavages were allowed and included. Carbamidomethylation of cysteine was allowed as constant modification; acetylation of the N terminus of the protein, pyroglutamate formation from N terminal glutamine, and oxidation of methionine were allowed as variable modifications. The number of modifications was limited to two per peptide. Protein Prospector thresholds used for identification criteria were: minimal protein score of 15, minimal peptide score of 15, maximum expectation value of 0.1, and minimal discriminant score threshold of 0.0. The false discovery rate was limited to 1%. Protein hits were considered significant when two or more peptide sequences matched a protein entry. Further details about identification of fragments and criteria used have been described by us elsewhere (Clauser *et al.*, 1999).

Measurement of intracellular calcium $[Ca^{2+}]_i$

Transfected HEK293 cells were grown on 96-well plates (25,000 cells were seeded per well; 3–4 wells per condition were used). AT 48 h posttransfection, cells were loaded with Fura-2AM, and $[Ca^{2+}]_i$ was measured as described previously (Hasdemir *et al.*, 2012). Agonist-induced peak Ca^{2+} responses were normalized to peak ionomycin-induced responses. Cells were stimulated with 1 µM ionomycin 90 s after agonist (100 nM) stimulation, as indicated in the example Ca^{2+} traces in Figure 3F.

cAMP measurements

Two methods were used for cAMP measurements. The cAMP data shown in Figure 3E were derived as follows: full-length, untagged $CRF_2\beta R$ or FLAG-$CRF_2\beta R\Delta SP$ constructs were transfected

individually in HEK293 cells grown on poly-D-lysine–coated six-well plates. Cellular cAMP levels were measured by using Perkin Elmer Lance TR-FRET based cAMP assay kits and 96-well white optiplates (Perkin Elmer, Cambridge, UK). Briefly, 48 h following transfection, cells were removed with 0.25% (wt/vol) trypsin containing 0.53 mM EDTA solution, washed with PBS, and resuspended in assay stimulation buffer (PBS with 0.1% BSA and 0.5 mM IBMX). The cells were counted with a hemocytometer, and the appropriate cell number was pelleted at 500 × *g* for 4 min and resuspended in stimulation buffer with 1/100 Alexa Fluor 647 anti-cAMP antibody at an assay concentration of 2000 cells/10 µl. Cells were loaded onto a 96-well white optiplate and were stimulated in triplicate with 30 and 100 nM of Ucn1 or Ucn2. The plate was incubated in the absence of light for 30 min before 20 µl/well of detection mix was added. The plate was incubated in the dark for a further 60 min. FRET was recorded by excitation at 320 nm and emission at 665 nm, using an EnVision Xcite multilabel plate reader (Perkin Elmer, Cambridge, UK).

The cAMP data shown in Figure 6, C and D, were derived as follows: individually transfected (CRF_1R or $CRF_2\beta R\Delta SP$) and cotransfected (CRF_1R+$CRF_2\beta R\Delta SP$) HEK293 cells were grown on poly-D-lysine–coated 12-well plates and challenged with agonist (100 nM CRF, Ucn1, Ucn2, or CRF+Ucn2) or vehicle (giving basal levels). Cells were then washed with ice-cold PBS and solubilized with 0.1 M HCl/0.1% Triton X-100. The lysates were used to measure levels of cAMP with a competitive immunoassay kit (Direct cAMP ELISA Kit; Enzo Life Sciences, Farmingdale, NY) according to the manufacturer's guidelines. All cAMP concentrations were corrected for protein levels (5 µg of protein per well were used in the enzyme-linked immunosorbent assay). Results are expressed as fold increase over basal.

Statistical analysis

Data are presented as mean ± SEM from $n \geq 3$ experiments. Prism (GraphPad Software, San Diego, CA) was used for statistical analysis. When comparing multiple groups, one-way analysis of variance (ANOVA) followed by post hoc Tukey's multiple comparisons was used. When two groups were compared, Student's *t* test was used. $p < 0.05$ was considered significant.

ACKNOWLEDGMENTS

We thank Mai Nguyen for her help in making the HA-tagged $CRF_2\beta R$ construct. M.W. is a Warwick Medical School Doctoral Training Centre in Interdisciplinary Biomedical Research student. This work was supported by National Institutes of Health grants GM8P41GM103481 to A. Burlingame and DK080787 to A. Bhargava. B.H. was in part supported by T32 AT003997 from the National Institutes of Health/National Center for Complementary and Integrative Health.

REFERENCES

Alken M, Rutz C, Kochl R, Donalies U, Oueslati M, Furkert J, Wietfeld D, Hermosilla R, Scholz A, Beyermann M, *et al*. (2005). The signal peptide of the rat corticotropin-releasing factor receptor 1 promotes receptor expression but is not essential for establishing a functional receptor. Biochem J 390, 455–464.

Bhargava A (2011). CRF and urocortins: a challenging interaction between family members. Gastroenterology 140, 1391–1394.

Binda AV, Kabbani N, Lin R, Levenson R (2002). D2 and D3 dopamine receptor cell surface localization mediated by interaction with protein 4.1N. Mol Pharmacol 62, 507–513.

Bockaert J, Fagni L, Dumuis A, Marin P (2004). GPCR interacting proteins (GIP). Pharmacol Ther 103, 203–221.

Boulant S, Kural C, Zeeh JC, Ubelmann F, Kirchhausen T (2011). Actin dynamics counteract membrane tension during clathrin-mediated endocytosis. Nat Cell Biol 13, 1124–1131.

Chang J, Adams MR, Clifton MS, Liao M, Brooks JH, Hasdemir B, Bhargava A (2011). Urocortin 1 modulates immunosignaling in a rat model of colitis via corticotropin-releasing factor receptor 2. Am J Physiol Gastrointest Liver Physiol 300, G884–G894.

Chrousos GP (2009). Stress and disorders of the stress system. Nat Rev Endocrinol 5, 374–381.

Clauser KR, Baker P, Burlingame AL (1999). Role of accurate mass measurement (+/– 10 ppm) in protein identification strategies employing MS or MS/MS and database searching. Anal Chem 71, 2871–2882.

Cornea-Hebert V, Watkins KC, Roth BL, Kroeze WK, Gaudreau P, Leclerc N, Descarries L (2002). Similar ultrastructural distribution of the 5-HT(2A) serotonin receptor and microtubule-associated protein MAP1A in cortical dendrites of adult rat. Neuroscience 113, 23–35.

Doyon C, Moraru A, Richard D (2004). The corticotropin-releasing factor system as a potential target for antiobesity drugs. Drug News Perspect 17, 505–517.

Gao F, Harikumar KG, Dong M, Lam PC, Sexton PM, Christopoulos A, Bordner A, Abagyan R, Miller LJ (2009). Functional importance of a structurally distinct homodimeric complex of the family B G protein-coupled secretin receptor. Mol Pharmacol 76, 264–274.

Gao MH, Giamouridis D, Lai NC, Walenta E, Paschoal VA, Kim YC, Miyanohara A, Guo T, Liao M, Liu L, *et al*. (2016). One-time injection of AAV8 encoding urocortin 2 provides long-term resolution of insulin resistance. JCI Insight 1, e88322.

Gingras AC, Aebersold R, Raught B (2005). Advances in protein complex analysis using mass spectrometry. J Physiol 563, 11–21.

Gottlieb TA, Ivanov IE, Adesnik M, Sabatini DD (1993). Actin microfilaments play a critical role in endocytosis at the apical but not the basolateral surface of polarized epithelial cells. J Cell Biol 120, 695–710.

Grammatopoulos DK (2012). Insights into mechanisms of corticotropin-releasing hormone receptor signal transduction. Br J Pharmacol 166, 85–97.

Grammatopoulos DK, Randeva HS, Levine MA, Katsanou ES, Hillhouse EW (2000). Urocortin, but not corticotropin-releasing hormone (CRH), activates the mitogen-activated protein kinase signal transduction pathway in human pregnant myometrium: an effect mediated via R1alpha and R2beta CRH receptor subtypes and stimulation of Gq-proteins. Mol Endocrinol 14, 2076–2091.

Guan S, Price JC, Prusiner SB, Ghaemmaghami S, Burlingame AL (2011). A data processing pipeline for mammalian proteome dynamics studies using stable isotope metabolic labeling. Mol Cell Proteomics 10, M111 010728.

Harikumar KG, Morfis MM, Lisenbee CS, Sexton PM, Miller LJ (2006). Constitutive formation of oligomeric complexes between family B G protein-coupled vasoactive intestinal polypeptide and secretin receptors. Mol Pharmacol 69, 363–373.

Hasdemir B, Bunnett NW, Cottrell GS (2007). Hepatocyte growth factor-regulated tyrosine kinase substrate (HRS) mediates post-endocytic trafficking of protease-activated receptor 2 and calcitonin receptor-like receptor. J Biol Chem 282, 29646–29657.

Hasdemir B, Mahajan S, Bunnett NW, Liao M, Bhargava A (2012). Endothelin-converting enzyme-1 actions determine differential trafficking and signaling of corticotropin-releasing factor receptor 1 at high agonist concentrations. Mol Endocrinol 26, 681–695.

Henckens MJ, Deussing JM, Chen A (2016). Region-specific roles of the corticotropin-releasing factor-urocortin system in stress. Nat Rev Neurosci 17, 636–651.

Hotta M, Shibasaki T, Arai K, Demura H (1999). Corticotropin-releasing factor receptor type 1 mediates emotional stress-induced inhibition of food intake and behavioral changes in rats. Brain Res 823, 221–225.

Kalwat MA, Thurmond DC (2013). Signaling mechanisms of glucose-induced F-actin remodeling in pancreatic islet beta cells. Exp Mol Med 45, e37.

Kim OJ, Ariano MA, Lazzarini RA, Levine MS, Sibley DR (2002). Neurofilament-M interacts with the D1 dopamine receptor to regulate cell surface expression and desensitization. J Neuroscience 22, 5920–5930.

Lai NC, Gao MH, Giamouridis D, Suarez J, Miyanohara A, Parikh J, Hightower S, Guo T, Dillmann W, Kim YC, *et al*. (2015). Intravenous AAV8 encoding urocortin-2 increases function of the failing heart in mice. Hum Gene Ther 26, 347–356.

Lamaze C, Fujimoto LM, Yin HL, Schmid SL (1997). The actin cytoskeleton is required for receptor-mediated endocytosis in mammalian cells. J Biol Chem 272, 20332–20335.

Levoye A, Dam J, Ayoub MA, Guillaume JL, Jockers R (2006). Do orphan G-protein-coupled receptors have ligand-independent functions? New insights from receptor heterodimers. EMBO Rep 7, 1094–1098.

Lewis K, Li C, Perrin MH, Blount A, Kunitake K, Donaldson C, Vaughan J, Reyes TM, Gulyas J, Fischer W, *et al.* (2001). Identification of urocortin III, an additional member of the corticotropin-releasing factor (CRF) family with high affinity for the CRF2 receptor. Proc Natl Acad Sci USA 98, 7570–7575.

Magalhaes AC, Holmes KD, Dale LB, Comps-Agrar L, Lee D, Yadav PN, Drysdale L, Poulter MO, Roth BL, Pin JP, *et al.* (2010). CRF receptor 1 regulates anxiety behavior via sensitization of 5-HT2 receptor signaling. Nat Neurosci 13, 622–629.

Mahajan S, Liao M, Barkan P, Takahashi K, Bhargava A (2014). Urocortin 3 expression at baseline and during inflammation in the colon: corticotropin releasing factor receptors cross-talk. Peptides 54, 58–66.

Margeta-Mitrovic M, Jan YN, Jan LY (2000). A trafficking checkpoint controls GABA(B) receptor heterodimerization. Neuron 27, 97–106.

Markovic D, Lehnert H, Levine MA, Grammatopoulos DK (2008). Structural determinants critical for localization and signaling within the seventh transmembrane domain of the type 1 corticotropin releasing hormone receptor: lessons from the receptor variant R1d. Mol Endocrinol 22, 2505–2519.

Markovic D, Vatish M, Gu M, Slater D, Newton R, Lehnert H, Grammatopoulos DK (2007). The onset of labor alters corticotropin-releasing hormone type 1 receptor variant expression in human myometrium: putative role of interleukin-1beta. Endocrinology 148, 3205–3213.

Milligan G (2009). G protein-coupled receptor hetero-dimerization: contribution to pharmacology and function. Br J Pharmacol 158, 5–14.

Muglia L, Jacobson L, Dikkes P, Majzoub JA (1995). Corticotropin-releasing hormone deficiency reveals major fetal but not adult glucocorticoid need. Nature 373, 427–432.

Murat B, Devost D, Andres M, Mion J, Boulay V, Corbani M, Zingg HH, Guillon G (2012). V1b and CRHR1 receptor heterodimerization mediates synergistic biological actions of vasopressin and CRH. Mol Endocrinol 26, 502–520.

Neufeld-Cohen A, Tsoory MM, Evans AK, Getselter D, Gil S, Lowry CA, Vale WW, Chen A (2010). A triple urocortin knockout mouse model reveals an essential role for urocortins in stress recovery. Proc Natl Acad Sci USA 107, 19020–19025.

O'Callaghan DW, Hasdemir B, Leighton M, Burgoyne RD (2003). Residues within the myristoylation motif determine intracellular targeting of the neuronal Ca^{2+} sensor protein KChIP1 to post-ER transport vesicles and traffic of Kv4 K^+ channels. J Cell Sci 116, 4833–4845.

Pal K, Swaminathan K, Xu HE, Pioszak AA (2010). Structural basis for hormone recognition by the Human CRFR2α G protein-coupled receptor. J Biol Chem 285, 40351–40361.

Paul NR, Allen JL, Chapman A, Morlan-Mairal M, Zindy E, Jacquemet G, Fernandez Del Ama L, Ferizovic N, Green DM, Howe JD, *et al.* (2015). α5β1 integrin recycling promotes Arp2/3-independent cancer cell invasion via the formin FHOD3. J Cell Biol 210, 1013–1031.

Perrin MH, DiGruccio MR, Koerber SC, Rivier JE, Kunitake KS, Bain DL, Fischer WH, Vale WW (2003). A soluble form of the first extracellular domain of mouse type 2β corticotropin-releasing factor receptor reveals differential ligand specificity. J Biol Chem 278, 15595–15600.

Reisine T, Rougon G, Barbet J, Affolter HU (1985). Corticotropin-releasing factor-induced adrenocorticotropin hormone release and synthesis is blocked by incorporation of the inhibitor of cyclic AMP-dependent protein kinase into anterior pituitary tumor cells by liposomes. Proc Natl Acad Sci USA 82, 8261–8265.

Reyes TM, Lewis K, Perrin MH, Kunitake KS, Vaughan J, Arias CA, Hogenesch JB, Gulyas J, Rivier J, Vale WW, Sawchenko PE (2001). Urocortin II: a member of the corticotropin-releasing factor (CRF) neuropeptide family that is selectively bound by type 2 CRF receptors. Proc Natl Acad Sci USA 98, 2843–2848.

Rodbell M (1995). Nobel Lecture. Signal transduction: evolution of an idea. Biosci Rep 15, 117–133.

Rosenfeld J, Capdevielle J, Guillemot JC, Ferrara P (1992). In-gel digestion of proteins for internal sequence analysis after one- or two-dimensional gel electrophoresis. Anal Biochem 203, 173–179.

Rutz C, Renner A, Alken M, Schulz K, Beyermann M, Wiesner B, Rosenthal W, Schulein R (2006). The corticotropin-releasing factor receptor type 2a contains an N-terminal pseudo signal peptide. J Biol Chem 281, 24910–24921.

Schulz K, Rutz C, Westendorf C, Ridelis I, Vogelbein S, Furkert J, Schmidt A, Wiesner B, Schulein R (2010). The pseudo signal peptide of the corticotropin-releasing factor receptor type 2a decreases receptor expression and prevents Gi-mediated inhibition of adenylyl cyclase activity. J Biol Chem 285, 32878–32887.

Sexton PM, Morfis M, Tilakaratne N, Hay DL, Udawela M, Christopoulos G, Christopoulos A (2006). Complexing receptor pharmacology: modulation of family B G protein-coupled receptor function by RAMPs. Ann NY Acad Sci 1070, 90–104.

Singh VP, Saluja AK, Bhagat L, Hietaranta AJ, Song A, Mykoniatis A, Van Acker GJ, Steer ML (2001). Serine protease inhibitor causes F-actin redistribution and inhibition of calcium-mediated secretion in pancreatic acini. Gastroenterology 120, 1818–1827.

Springael JY, Urizar E, Costagliola S, Vassart G, Parmentier M (2007). Allosteric properties of G protein-coupled receptor oligomers. Pharmacol Ther 115, 410–418.

Teichmann A, Gibert A, Lampe A, Grzesik P, Rutz C, Furkert J, Schmoranzer J, Krause G, Wiesner B, Schulein R (2014). The specific monomer/dimer equilibrium of the corticotropin-releasing factor receptor type 1 is established in the endoplasmic reticulum. J Biol Chem 289, 24250–24262.

Teichmann A, Rutz C, Kreuchwig A, Krause G, Wiesner B, Schulein R (2012). The pseudo signal peptide of the corticotropin-releasing factor receptor type 2A prevents receptor oligomerization. J Biol Chem 287, 27265–27274.

Trester-Zedlitz M, Burlingame A, Kobilka B, von Zastrow M (2005). Mass spectrometric analysis of agonist effects on posttranslational modifications of the beta-2 adrenoceptor in mammalian cells. Biochemistry 44, 6133–6143.

Vaughan J, Donaldson C, Bittencourt J, Perrin MH, Lewis K, Sutton S, Chan R, Turnbull AV, Lovejoy D, Rivier C, *et al.* (1995). Urocortin, a mammalian neuropeptide related to fish urotensin I and to corticotropin-releasing factor. Nature 378, 287–292.

Vischer HF, Castro M, Pin JP (2015). G protein-coupled receptor multimers: a question still open despite the use of novel approaches. Mol Pharmacol 88, 561–571.

Vischer HF, Watts AO, Nijmeijer S, Leurs R (2011). G protein-coupled receptors: walking hand-in-hand, talking hand-in-hand. Br J Pharmacol 163, 246–260.

Zhao GQ, Zhang Y, Hoon MA, Chandrashekar J, Erlenbach I, Ryba NJ, Zuker CS (2003). The receptors for mammalian sweet and umami taste. Cell 115, 255–266.